

Earth's Future

RESEARCH ARTICLE

10.1029/2023EF004102

National-Scale Rainfall-Triggered Landslide Susceptibility and Exposure in Nepal



Key Points:

- Landslide susceptibility and population distribution generate highly spatially variable exposure to landslides across Nepal
- 44% of land in Nepal has moderate-high landslide susceptibility, whilst <15% of the population has moderate-high exposure to landsliding
- Caution is needed in using short-term landslide occurrence data to assess future risks due to rapidly changing susceptibility and exposure

Supporting Information:

Supporting Information may be found in the online version of this article.

Correspondence to:

M. E. Kinney,
mark.kinney@newcastle.ac.uk

Citation:

Kinney, M. E., Rosser, N. J., Swirad, Z. M., Robinson, T. R., Shrestha, R., Pujara, D. S., et al. (2024). National-scale rainfall-triggered landslide susceptibility and exposure in Nepal. *Earth's Future*, 12, e2023EF004102. <https://doi.org/10.1029/2023EF004102>

Received 13 SEP 2023

Accepted 7 JAN 2024

Author Contributions:

Conceptualization: M. E. Kinney, N. J. Rosser, Z. M. Swirad, T. R. Robinson, R. Shrestha, D. S. Pujara, G. K. Basyal, A. L. Densmore, K. Arrell, K. J. Oven, A. Dunant

Data curation: M. E. Kinney, N. J. Rosser, Z. M. Swirad

Formal analysis: M. E. Kinney, N. J. Rosser, Z. M. Swirad, T. R. Robinson, R. Shrestha, D. S. Pujara

Funding acquisition: N. J. Rosser, T. R. Robinson, A. L. Densmore, K. J. Oven

M. E. Kinney¹ , N. J. Rosser² , Z. M. Swirad³ , T. R. Robinson⁴, R. Shrestha⁵, D. S. Pujara⁵ , G. K. Basyal⁵, A. L. Densmore², K. Arrell⁶, K. J. Oven⁶, and A. Dunant²

¹School of Geography, Politics and Sociology, Newcastle University, Newcastle upon Tyne, UK, ²Department of Geography and Institute of Hazard Risk and Resilience, Durham University, Durham, UK, ³Institute of Geophysics, Polish Academy of Sciences, Warsaw, Poland, ⁴School of Earth and Environment, University of Canterbury, Canterbury, New Zealand, ⁵National Society for Earthquake Technology, Kathmandu, Nepal, ⁶Department of Geography and Environmental Sciences, Northumbria University, Newcastle upon Tyne, UK

Abstract Nepal is one of the most landslide-prone countries in the world, with year-on-year impacts resulting in loss of life and imposing a chronic impediment to sustainable livelihoods. Living with landslides is a daily reality for an increasing number of people, so establishing the nature of landslide hazard and risk is essential. Here we develop a model of landslide susceptibility for Nepal and use this to generate a nationwide geographical profile of exposure to rainfall-triggered landslides. We model landslide susceptibility using a fuzzy overlay approach based on freely-available topographic data, trained on an inventory of mapped landslides, and combine this with high resolution population and building data to describe the spatial distribution of exposure to landslides. We find that whilst landslide susceptibility is highest in the High Himalaya, exposure is highest within the Middle Hills, but this is highly spatially variable and skewed to on average relatively low values. Around 4×10^6 Nepalis (~15% of the population) live in areas considered to be at moderate or higher degree of exposure to landsliding (>0.25 of the maximum), and critically this number is highly sensitive to even small variations in landslide susceptibility. Our results show a complex relationship between landslides and buildings, that implies wider complexity in the association between physical exposure to landslides and poverty. This analysis for the first time brings into focus the geography of the landslide exposure and risk case load in Nepal, and demonstrates limitations of assessing future risk based on limited records of previous events.

Plain Language Summary Mountain region populations are disproportionately impacted by landslide hazards that result in seasonal disruption and loss of life, and restrict longer-term sustainable development opportunities. Crucially, effective management of landslide risk requires an understanding of both where landslides are likely to occur but also how they intersect with where people live. To address this, we use a numerical model to identify locations that are more likely to experience landsliding in the future, based on a map of where landslides have occurred in the past. We then combine this with population and building data to consider how people's exposure to landsliding varies across Nepal. We find that although landslides are most likely within the higher mountain areas, the low population numbers here mean that people's exposure to landsliding is relatively limited. Similarly, the higher population centers are typically in areas where landsliding is less likely to occur. Locations with relatively high exposure instead generally occur in isolated pockets at the intersection between landslide likelihood and population density within moderate relief areas of Nepal. Understanding this spatial variability in landslide exposure is important for informing future risk-sensitive land use planning and resource allocation.

1. Introduction

Mountain regions worldwide occupy >27% of the Earth's land surface and are home to >1 bn people (14% of the world's population) (Ehrlich et al., 2021). Steep and often unstable slopes can pose immense challenges to their inhabitants, with mountain-region countries witnessing >70% of reported disaster-related deaths between 2005 and 2014 (Klein et al., 2019; UNISDR, 2015). These statistics likely under-represent losses from recurrent, often highly localized mass movements (Froude & Petley, 2018), which also act as impediments to sustainable livelihoods and wider mountain-region development (Arouri et al., 2015; Gerrard & Gardner, 2002; Tobin et al., 2011; Wymann von Dach et al., 2017). Nepal is a global hotspot for mountain hazards and is one of the most

© 2024 The Authors. Earth's Future published by Wiley Periodicals LLC on behalf of American Geophysical Union. This is an open access article under the terms of the [Creative Commons Attribution License](https://creativecommons.org/licenses/by/4.0/), which permits use, distribution and reproduction in any medium, provided the original work is properly cited.

Investigation: M. E. Kincey, N. J. Rosser, Z. M. Swirad, T. R. Robinson, R. Shrestha, D. S. Pujara

Methodology: M. E. Kincey, N. J. Rosser, Z. M. Swirad, T. R. Robinson

Project administration: N. J. Rosser

Software: M. E. Kincey, N. J. Rosser, Z. M. Swirad, T. R. Robinson

Visualization: M. E. Kincey, N. J. Rosser, Z. M. Swirad, T. R. Robinson

Writing – original draft: M. E. Kincey, N. J. Rosser, Z. M. Swirad, T. R. Robinson

Writing – review & editing:

M. E. Kincey, N. J. Rosser, Z. M. Swirad, T. R. Robinson, A. L. Densmore, K. Arrell, K. J. Oven, A. Dunant

landslide-prone countries in the world (Dilley et al., 2005; Petley et al., 2007), with >10% of global rainfall-triggered fatal landslides despite having <0.4% of the global population (Froude & Petley, 2018). Losses are manifest in a recurrent seasonal pattern that approximately tracks the annual monsoon (Petley, 2012), and these losses have continued despite efforts to reduce their long-recognised impacts (e.g., Eckholm, 1975). Importantly, people's lived experience of landslides and landslide impacts varies considerably through the year and from place to place in Nepal (Oven et al., 2021; Rosser et al., 2021), and so identifying the footprint of landslide risk is essential to guide any form of mitigation.

Mountain regions are also currently experiencing rapid land use change (Wester et al., 2019), further raising concerns. Mountain populations grew by 16% between 2000 and 2012 (Ehrlich et al., 2021), and a combination of increasing concentrations in (peri-)urban mountain areas and associated unregulated road construction place more people in locations where landslide hazards may be experienced (McAdoo et al., 2018; Rusk et al., 2022). Demand for safe habitable land can be acute (e.g., Smyth & Royle, 2000), and where such land is available, it is often only separated by a short distance from areas deemed hazardous (Zimmermann & Keiler, 2015). Mountains are also highly susceptible to climate change. For example, the intensification of the South Asian Monsoon (Kitoh, 2017) and an increased frequency of extreme rainfall (McSweeney et al., 2012) combined are likely to lead to future increases in landslide hazard. Characterizing present-day landslide risk is therefore essential as a benchmark for future appraisals of change (Jakub, 2021), as living with landslides is both now, and will increasingly be, a daily reality for many (Cieslik et al., 2019; Oven, 2009).

For the purposes of this study, we use the standard disaster-related terminology as defined by the United Nations Office for Disaster Risk Reduction (UNDRR) as part of the Sendai Framework (<https://www.undrr.org/terminology#R>). A *hazard* is defined as “a process, phenomenon or human activity that may cause loss of life, injury or other health impacts, property damage, social and economic disruption or environmental degradation.” *Exposure* relates to “the situation of people, infrastructure, housing, production capacities and other tangible human assets located in hazard-prone areas.” *Risk* is then “the potential loss of life, injury, or destroyed or damaged assets,” which is determined as the intersection between hazard, exposure, vulnerability and capacity. We define *impact* as the realisation of landslide risk in terms of actual recorded landslide incidents.

In mountain regions, the geographical distributions of landslide hazard (here represented by landslide *susceptibility*, defined as the likelihood of a landslide occurring in a given area (Reichenbach et al., 2018)) and population determine the overall *exposure to landslides*, and this can vary significantly (Corominas et al., 2014; Emberson et al., 2020). People's exposure to landslides may vary as a result of either deliberate or unintentional decision-making (e.g., Gentle & Maraseni, 2012; Glade & Crozier, 2005), and/or more formal risk-averse land-use planning strategies (e.g., Fuchs et al., 2015; Persichillo et al., 2017). Further, increased landslide exposure may result from people being forced to occupy more landslide-prone land, often as a result of poverty and marginalization (e.g., Rieger, 2021); or occupying higher risk locations though limited or constrained choice (Oven & Rigg, 2015). It is clear that risk can be further exacerbated by changes in either exposure (e.g., due to road-side settlements; Lennartz, 2013) or landslide hazard (e.g., after large earthquakes; Rosser et al., 2021).

When assessed at regional or national scale, landslide susceptibility and exposure in some mountainous regions can appear to “saturate” at high and seemingly intolerable levels, generating apparently ubiquitous presentations of risk at the intersection between even moderate susceptibilities and population densities (Ozturk et al., 2021). However, as both landslide susceptibility and population density vary significantly over small distances (as little as 10s of m), it is essential to characterize their geography in detail to ensure that such assessments are accurate and useful, and available at the scale at which landslides are experienced and mitigation decisions are made (Oven et al., 2021). Where past observations of landslide occurrence are absent or incomplete, modeling landslide susceptibility and exposure to identify hotspots or to extend awareness of landslides over uncharted areas must be a priority (Guzzetti et al., 2005). Further, as increasing trends in losses due to landslides emerge (Froude & Petley, 2018; Petley et al., 2007), it also remains essential to distinguish any change in landslide activity from other drivers of risk, such as population growth or policy interventions (Huggel et al., 2015; Machado et al., 2021; Petley et al., 2007).

The number of statistical landslide susceptibility models has substantially increased during recent years (Reichenbach et al., 2018), including in low- to middle-income countries, in part enabled by increasingly open access to both data and processing capabilities (Fleuchaus et al., 2021). Yet the utility of many of these models

remains limited by the quality of the data on which they are trained and validated. A similar proliferation has been seen in the collation of landslide impact data (e.g., fatalities, injuries), with examples such as the BIPAD disaster information management system in Nepal (<https://bipadportal.gov.np/>; Neupane, 2020). Whilst these data are essential for profiling risks and their impact, their interpretation and extrapolation need to be undertaken with care until the completeness, duration, and potential bias of such records can be fully considered (Huggel et al., 2015; Kirschbaum et al., 2010). The statistical analysis of landslide risk (posed to people, buildings, infrastructure), beyond susceptibility alone, still attracts relatively limited attention (Petschko et al., 2014) due to the need to combine hazard, vulnerability and exposure. This presents a critical gap, where recorded historical impacts are often used to model or validate estimates of future landslide *risk* (e.g., Rusk et al., 2022; Stanley & Kirschbaum, 2017). Whilst ultimately it is the *impacts* which need to be mitigated, equating *impact* to *risk* is problematic, which we explore further below in our focus on physical exposure to landslides.

In this paper, we develop and integrate landslide susceptibility and population data to generate a pattern of rainfall-triggered landslide exposure across Nepal. We restrict our analysis to a consideration of exposure to landslides as the extension of this to *landslide risk* remains problematic in the absence of sufficiently granular vulnerability data. We model landslide susceptibility using a fuzzy overlay approach based on a high-resolution nationwide topographic data set, trained on an inventory of mapped rainfall-triggered landslides reported by Kinsey et al. (2021). Fuzzy logic-based models are computationally simple yet can incorporate large input data uncertainties and have been shown to provide spatially accurate representations of landslide susceptibility (Kritikos et al., 2015; Robinson et al., 2017), often outperforming other statistical modeling techniques (Bui et al., 2012; Pourghasemi et al., 2012). We use population and building data to construct national exposure models at 90 m resolution. We explore these models to consider the spatial and demographic patterns of who is exposed to landslides in Nepal, and to assess the degree to which short-term impact data sets may not be sufficient to understand emerging landslide risks due to changes in settlement and development.

2. Materials and Methods

2.1. Landslide and Topography Data

We developed a nationwide landslide susceptibility model (Figure 1) trained on 6,731 mapped landslides sampled from 14 districts (22,774.59 km²/15.42% of Nepal) in central Nepal during the period April 2014 to March 2015, prior to the 25 April 2015 Gorkha earthquake (see: Kinsey et al., 2021). These districts were chosen because they comprise the most complete available large-scale landslide inventory for Nepal. We excluded areas affected by cloud or snow cover from further analysis due to the ground being occluded (c. 8% of the mapped area). We used three independent epochs of landslide polygon data to mitigate the variability in landsliding associated with single-epoch inventories. Importantly, our approach to mapping also included the recording of all landslides visible on imagery from the three epochs, rather than just new landslides that occurred within the mapping time window, meaning that the inventory is representative of longer-term landslide occurrence within the study area. Landslide polygons included both source and deposit area. All mapped landslides are aseismic in origin, notwithstanding long-term (ca. centennial) earthquake legacy effects (e.g., Parker et al., 2015). Landslide polygons were rasterized at 30 m resolution covering 0.41% of the mapping area (84.7 km²; 94,079 total cells). We then randomly split the rasterized landslide inventory into equal training and test data sets on a cell-by-cell basis, with the former used to quantify the frequency distributions of topographic covariates and the latter to independently assess model performance via Area under the Receiver Operating Characteristic curve (AUROC).

We defined 10 covariates using topographic derivatives from the ALOS DEM at 30 m resolution. Each has previously been identified as a direct measure of, or proxy for, the controls on landsliding (e.g., Parker et al., 2015; Robinson et al., 2017), and has the advantage of being obtained from a single nationwide topographic data set. These were: (a) *elevation*, (b) *slope*, (c) *aspect*, (d) *normalized stream-ridge distance* (NSRD), (e) *planform curvature*, (f) *profile curvature*, (g) *hillslope relief* (standard deviation of elevation within a 900 m radius), (h) *local relief* (standard deviation of elevation within a 300 m radius), (i) *topographic wetness index* (TWI), and (j) *upslope contributing area* (UCA) (see: Text S1 in Supporting Information S1; Figure S1). We excluded covariates explicitly describing landslide triggering (e.g., precipitation) given the limited completeness and resolution of these data available at the nationwide scale, and because studies have shown that long-term precipitation

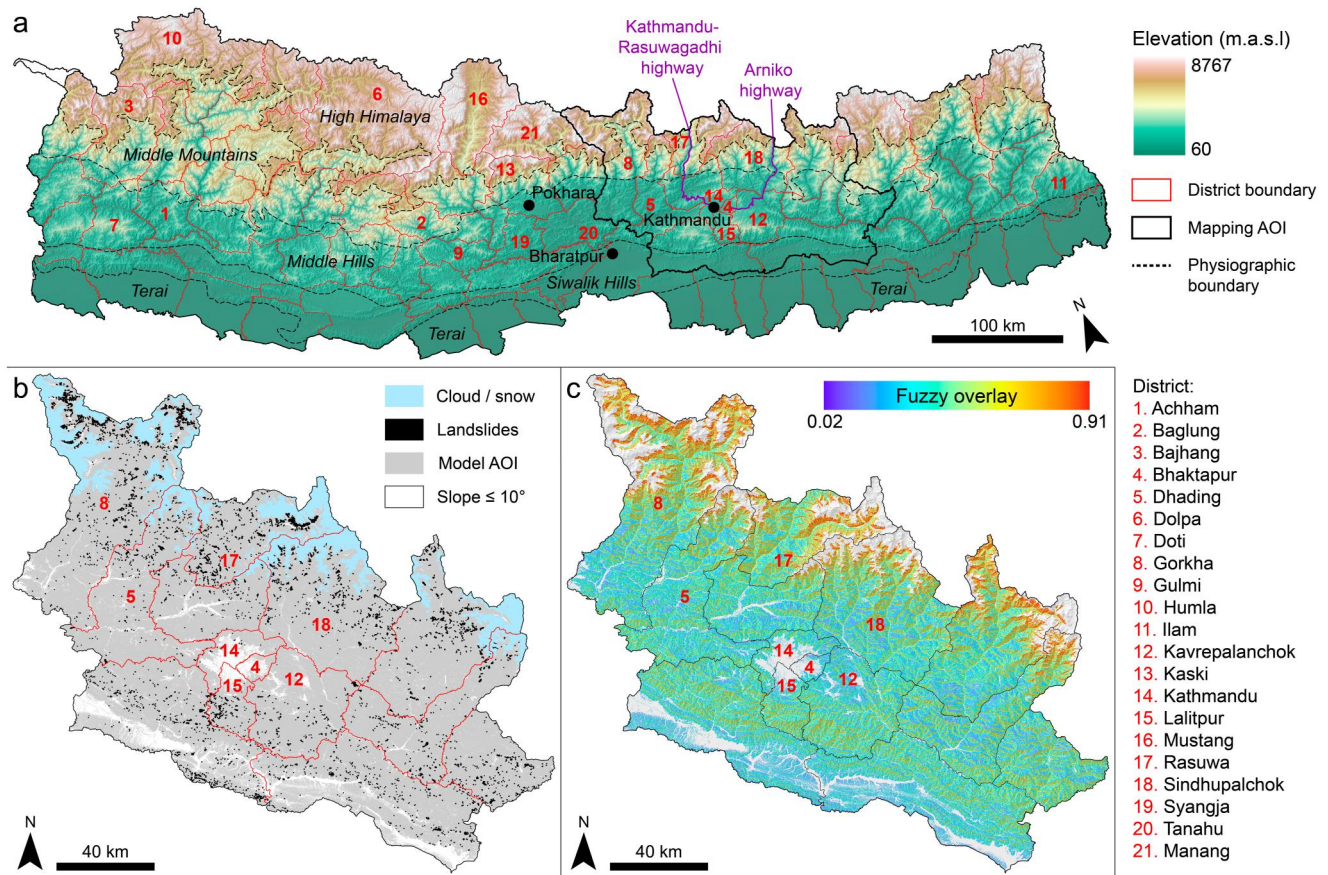


Figure 1. (a) Map of Nepal showing the main physiographic divisions, administrative (district) boundaries and major urban centers. The landslide mapping area, spanning 14 districts of central Nepal, is outlined in black. Districts referred to in the text are numbered in red. (b) Detail of the mapped area showing the distribution of identified landslide polygons from all three epochs. (c) Results of the six-variable fuzzy logic model, displayed as the distribution of fuzzy overlay scores. The underlying topographic data is a 30-m resolution ALOS digital elevation model (AW3D30 – JAXA).

patterns are not directly indicative of landslide densities (e.g., Kinney et al., 2021). Including the high intensity cloud-burst events that do typically cause landslides within the model is problematic due to the relative infrequency of these events and the spatial variability in where they occur or could plausibly occur in the future. Our output model therefore represents the static propensity for landslides if a sufficient trigger were to occur. In other words, our model is specifically designed to provide a national-scale indication of the long-term relative likelihood of landsliding due to rainfall events, and so is developed without the inclusion of a specific precipitation trigger factor.

We used morphometric proxies for geotechnical strength because data at a meaningful scale for individual slope stability are also unavailable, and other proxy data (e.g., coarse-resolution geological data) would otherwise introduce artificial spatial heterogeneity with limited relevance to slope stability (Gaidzik & Ramírez-Herrera, 2021; Reichenbach et al., 2018). We deliberately chose not to include land use or land cover data within the range of model factors as the functional links between such factors and landslide occurrence are complex and at times contradictory (cf. Carrara et al., 1991, 1995). Land cover and land use are also implicitly included within the topographic factors that we did include though, such as through the influence of elevation, slope and aspect on how a landscape is typically utilized and managed. This approach to susceptibility modeling based solely on topographic factors is common within the literature and reflects issues with the accuracy and completeness of other input data sets (Reichenbach et al., 2018) and the specific focus of our study. Importantly, we ensured that the distribution of the chosen covariates in the training area reflected the equivalent distribution across the area over which the model is extrapolated (Reichenbach et al., 2018). The only variable that showed divergence between the training area and the national distribution is *elevation* (Figure S2 in Supporting Information S1),

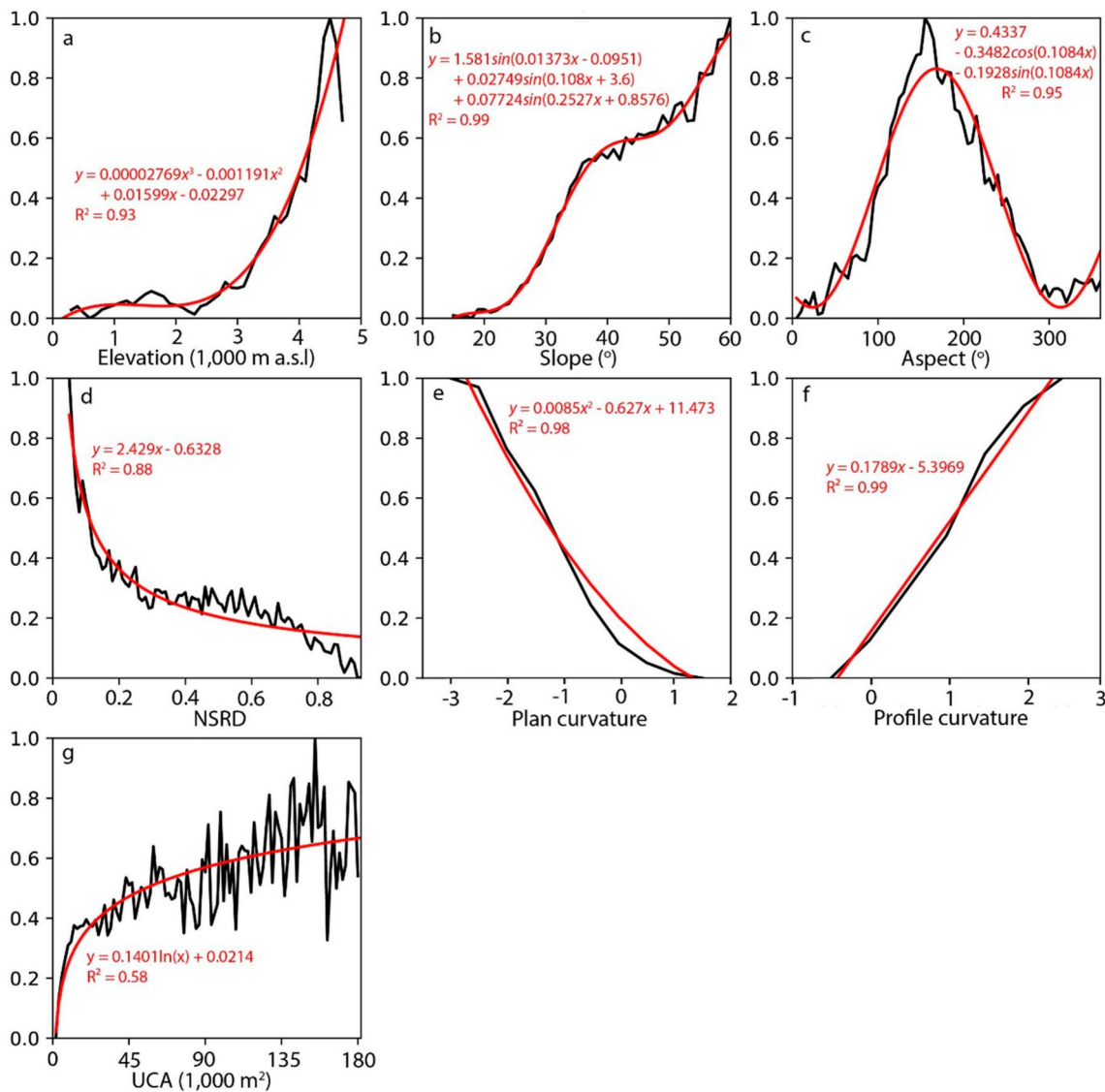


Figure 2. Normalized landslide frequency ratios (nLFR; black) and best-fit models (red) for the topographic covariates: (a) elevation, (b) slope, (c) aspect, (d) normalized stream-ridge distance (NSRD), (e) planform curvature (positive values indicate a laterally convex surface with divergent flow; negative values indicate a laterally concave surface with convergent flow), (f) profile curvature (positive values indicate an upwardly concave surface where flow is accelerated; negative values indicate an upwardly convex surface where flow is decelerated), (g) upslope contributing area (UCA). Note that the variable scale (x) refers to the raw variable values while in the equations x represents the bin value (Table S1 in Supporting Information S1).

reflecting the relatively higher frequency of moderate to high elevations across the middle hills in Western and Far Western Nepal, outside of our training area (see: Figure 1).

Initial analysis of the influence of topographic factors on landslide occurrence showed that the relationship of landslides with slope angle is virtually zero at $\sim 15^\circ$ and is zero at 10° (Figure 2b). This finding is consistent with a range of other studies that have demonstrated that slope angles $< 10\text{--}15^\circ$ have little to no influence on landsliding (e.g., Kritikos et al., 2015; Meunier et al., 2008; Robinson et al., 2017). We therefore applied a conservative slope threshold of 10-degrees and excluded these areas from all further analyses (equivalent to 9.67% of the 14-district training area; 22.66% of the total area of Nepal). Analysis of all 10 covariates showed collinearity between some variables, here defined as a correlation > 0.6 . *Slope*, *hillslope relief*, and *local relief* were strongly correlated ($r \geq 0.67$ at 95% confidence level; Figure S3 in Supporting Information S1) and so we excluded both relief metrics to avoid overestimating the importance of these strongly-correlated factors. Similarly, we excluded *TWI* from the analysis because of its strong correlation with *planform curvature* (Figure S3 in Supporting Information S1).

Table 1
AUROC Score for the 7-Covariate Model and When Covariates Are Removed One-By-One

Variables used	Variables removed	AUROC
Elevation, slope, aspect, NSRD, plan curvature, profile curvature, UCA	–	0.737
Elevation, slope, aspect, NSRD, plan curvature, UCA	Profile curvature	0.750
Elevation, slope, aspect, NSRD, profile curvature, UCA	Plan curvature	0.742
Elevation, slope, aspect, NSRD, plan curvature, profile curvature	UCA	0.738
Elevation, slope, NSRD, plan curvature, profile curvature, UCA	Aspect	0.733
Elevation, slope, aspect, plan curvature, profile curvature, UCA	NSRD	0.729
Slope, aspect, NSRD, plan curvature, profile curvature, UCA	Elevation	0.724
Elevation, aspect, NSRD, plan curvature, profile curvature, UCA	Slope	0.701

Note. Bold text shows best-fitting model by AUROC score.

2.2. Fuzzy Logic

We modeled rainfall-triggered landslide susceptibility using fuzzy logic, which can simulate high-complexity multi-factor systems despite large uncertainties. The method has previously been successfully used to model both earthquake- and rainfall-triggered landslide susceptibility in Nepal and globally (Kritikos et al., 2015; Robinson et al., 2017; Stanley & Kirschbaum, 2017), and has been shown to match or outperform other statistical modeling approaches (Pourghasemi et al., 2012; Pradhan, 2010). Fuzzy logic is based on fuzzy set theory and the concept of partial membership between an event (landslide) and a set (topographic covariate), where events have a degree of membership between 0 (no membership) and 1 (full membership) with different sets. In this way, each covariate can be converted from its raw values to a 0–1 scale showing the relative susceptibility of landslides occurring at those values (0: negligible; 1: high). Aggregating multiple different covariates together through fuzzy overlay produces a total relative landslide susceptibility score (0–1).

The critical step in fuzzy logic modeling is the derivation of the membership functions for each covariate. Here, we binned the topographic covariates using equal intervals, optimized to capture the difference in the relative proportion of landslides and no landslides for each interval, while smoothing small-scale noise (Table S1 in Supporting Information S1). We then used normalized landslide frequency ratios ($nLFR$) to evaluate the degree of membership between landslides and the different topographic covariates in each bin (Kritikos et al., 2015). Landslide frequency ratios (LFR) compare the relative frequency of landsliding for different values of a variable against the overall frequency of those values across the study area. LFR values > 1 show preferential occurrence at these values while LFR values < 1 show that fewer landslides occur for these values than expected. Raw LFR values were normalized between 0 and 1, allowing results for all topographic covariates to be directly compared. Fuzzy memberships were then created through a semi-data driven approach (Kritikos et al., 2015) by fitting curves to the $nLFR$ values via best fit models, evaluated using the coefficient of determination (R^2) (Figure 2).

We adopted the fuzzy gamma approach for aggregation as the most appropriate for modeling natural phenomena such as landslide susceptibility (Kritikos et al., 2015). Fuzzy gamma establishes the combined effect of multiple fuzzy memberships by:

$$L_{\text{Suscept}} = \left(1 - \prod_{S=1}^j (1 - \mu_S)\right)^\gamma \times \left(\prod_{S=1}^j \mu_S\right)^{1-\gamma} \quad (2)$$

where L_{Suscept} is the total landslide susceptibility score; μ_S is the fuzzy membership value for set S where $S = 1, 2, \dots, j$; j is the total number of sets (or covariates) to be aggregated; and γ is a user-defined parameter between 0 and 1. The selection of γ is critical to the final susceptibility values, with Kritikos and Davies (2015) showing that values < 0.9 better forecast landslide non-occurrence and values > 0.9 better forecast landslide occurrence but with large over-prediction rates. We set $\gamma = 0.9$ as a compromise between forecasting landslide occurrence and limiting over-prediction. We used the test landslide data set to evaluate the model via AUROC, where scores of 0.5 represent model performance no better than random, and scores > 0.7 were judged to be successful. We ran the initial model using all seven remaining covariates, and then performed a sensitivity analysis based on AUROC scores, removing each individual covariate to find the best performing model (Table 1). The best performing

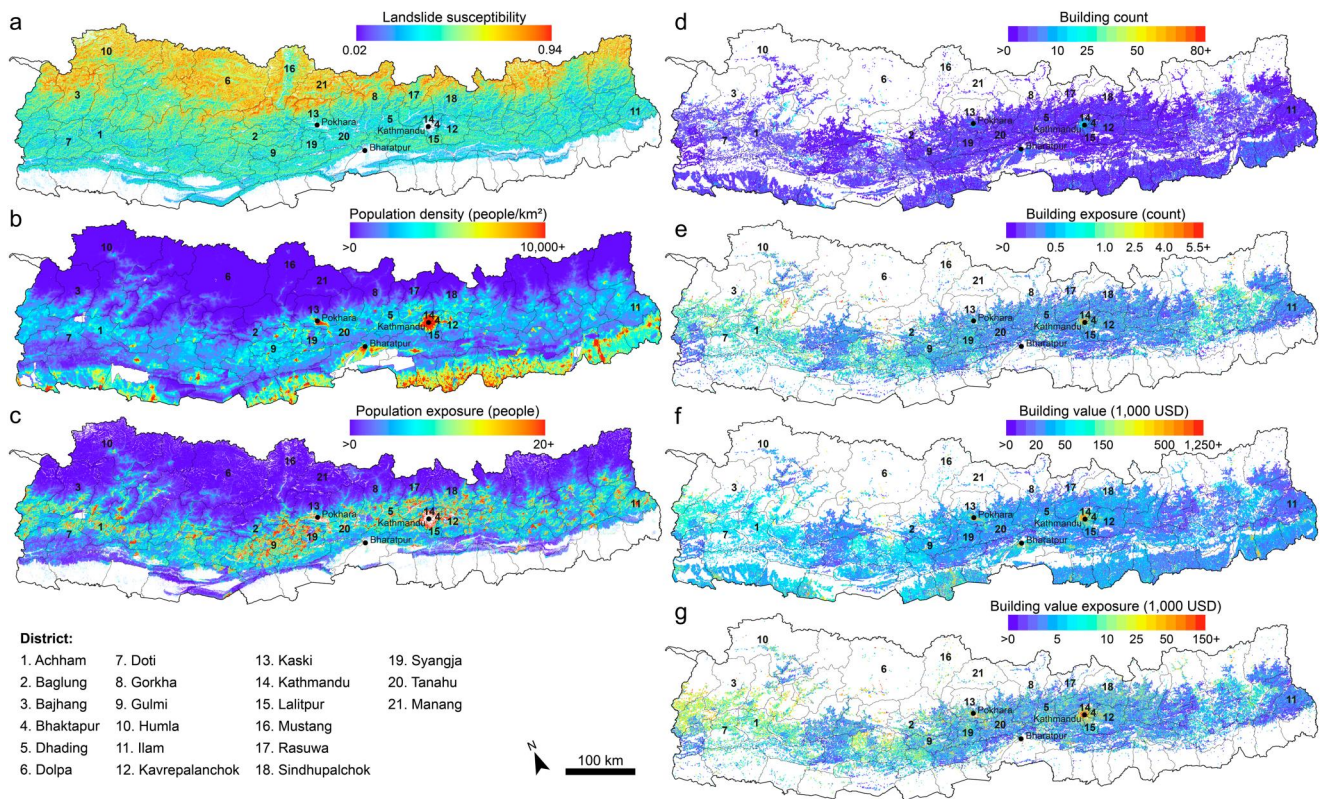


Figure 3. Distribution maps for Nepal showing: (a) the results of the six-variable fuzzy logic landslide susceptibility model considered the most successful (L_{suscept} , 90 m cell size); (b) population density based on the unconstrained UN-adjusted population data for 2011 from WorldPop (90 m); (c) measure of population exposure to landsliding ($L_{\text{suscept}} \times \text{population}$, 90 m); (d) total building count per cell from the METEOR project (90 m); (e) measure of building count exposure to landsliding ($L_{\text{suscept}} \times \text{building count}$, 90 m); (f) total building monetary value per cell from METEOR project (90 m); and (g) measure of building exposure to landsliding ($L_{\text{suscept}} \times \text{building value}$, 90 m). Note that the distributions of population exposure, building count exposure and building value exposure are markedly different from the individual distributions for landslide susceptibility, population density, building count and building value. For all maps, areas of no data or zero values are shown in gray.

model had an AUROC score of 0.75 and was derived from six variables: *elevation, slope, aspect, NSRD, plan curvature and UCA* (Figure 1c; Text S4 in Supporting Information S1), which we used to model landslide susceptibility nationwide (Figures 3a and 4a). The landslide susceptibility model has a value range of 0–1, with 1 representing the most susceptible locations within the study area. For our subsequent comparative analyses, we classify the data using breaks of 0.25, 0.5 and 0.75 to assess what proportion of the landscape has values within each quartile of the overall susceptibility range.

2.3. Population, Infrastructure, and Exposure

To evaluate the intersection of population and landsliding we consider spatial variability in both population density and building distribution. Assessment of population exposure requires understanding of where people reside at a comparable scale to the susceptibility data. To enable this, there have been several attempts to disaggregate census data, which are typically collated by local government unit, onto a regular grid (TReNDS, 2020). Here, we use the unconstrained UN-adjusted population data for Nepal in 2011 from WorldPop (2020), which is based on the disaggregation of census information from discrete administrative units to ~90 m grid population counts using Random Forest classification of a series of remotely sensed population covariates (Stevens et al., 2015; Tatem, 2017) (Figures 3b and 4b). 2011 is the most recent data set that coincided with a national census, thereby minimizing potential errors from forward projection of estimated growth rates. Our results are therefore specific to 2011 but are likely to reflect longer-term relative patterns of exposure.

The landslide susceptibility model L_{suscept} (30 m) was resampled to match the resolution of the WorldPop population count data, which for Nepal is at 90 m resolution. A measure of the population exposure to landsliding

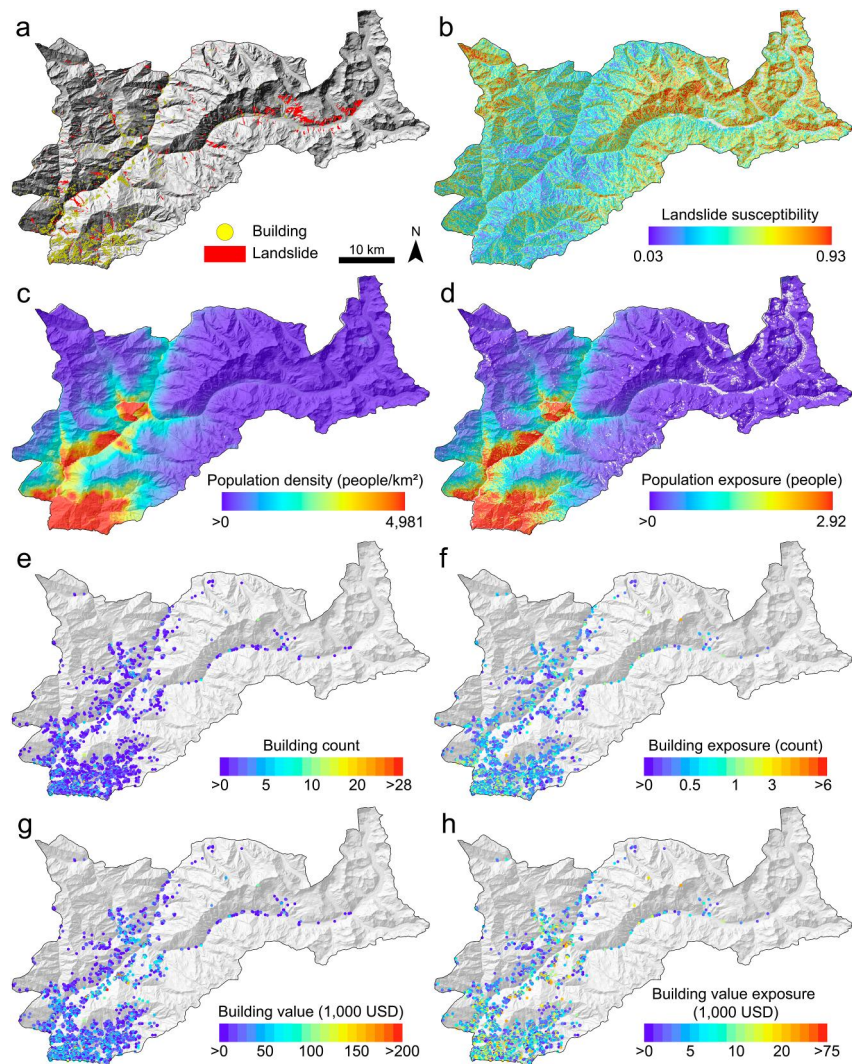


Figure 4. Maps showing an example of the detailed geography of the components of risk for Rasuwa district in north-central Nepal, including the distributions of (a) mapped landslides and building locations, (b) landslide susceptibility L_{suscept} , (c) population density, (d) measure of population exposure, (e) building count, (f) measure of building count exposure, (g) building value, and (h) measure of building value exposure. For all maps, areas of no data or zero values are shown in gray, with the underlying topographic data being a 30-m resolution ALOS digital elevation model (AW3D30 – JAXA). The location of Rasuwa is indicated on Figure 1.

was calculated by multiplying L_{suscept} by the population count data, again at 90 m resolution (Figures 3c and 4c), resulting in a population exposure raster with units representing the number of people exposed to landslides. This approach to calculating exposure as the overlay of susceptibility and socio-economic assets (e.g., population, buildings) has been used successfully in a number of other studies of landslide hazard (Embersson et al., 2020; Pellicani et al., 2014; Promper et al., 2015; Rusk et al., 2022). To assess longer-term change since 2011, we also integrate the results of the 2021 census of Nepal, which is currently only available as ward-level administrative demographic summaries (Government of Nepal, 2023). We utilize this more recent data to make comparisons between how the broad scale population count and distribution has changed over the 10-year period from 2011 to 2021, and to consider in general terms how this may have affected population exposure to landsliding.

Until recently, spatially explicit data on residential housing have been fragmentary (Keiler, 2004), which has limited the assessment of building exposure to geohazards to only large-scale administratively aggregated data. In Nepal, whilst updates to OpenStreetMap (OSM) data of individual house footprints have been rapid, questions remain around completeness particularly in more remote and rural areas (Khanal

et al., 2019). For this study, building exposure is therefore calculated using the monetary building value assessment generated by the Modeling Exposure Through Earth Observation Routines (METEOR) project (METEOR Project Consortium, 2020; <https://meteor-project.org/>). These data describe the total USD value of buildings within each raster cell, and were gridded to a 90 m resolution raster (Figures 3 and 4d) then multiplied with the 90 m susceptibility to obtain a measure of the asset exposure also at 90 m and with units of USD (Figures 3e and 4e). Whilst the METEOR data combines the values of residential and some non-residential buildings, the methodology is based on the semi-automated spreading of the number of buildings from census data across local administrative units and so is overwhelmingly dominated by residential buildings (Huyck et al., 2019).

We summarized the gridded susceptibility values by taking the mean over both ward ($n = 6,817$) and district ($n = 77$) areas (Figures S5 and S6 in Supporting Information S1). Total population and building exposure were represented as the sum of the values of exposure cells for each ward and district. Summarizing susceptibility and exposure data at ward level, the smallest unit of local government in Nepal, minimizes the influence of individual anomalous cell values while also aggregating to a unit of analysis relevant to local governmental decision-making (Oven et al., 2021). Districts represent the third tier of administrative subdivision in Nepal, and act as a coordinating body between the provincial and federal government and the local municipalities (*palikas*) and their ward-level subdivisions.

2.4. Comparison to Landslide Impacts

To assess the agreement between modeled exposure to landslides and published landslide impact data across Nepal, we used landslide incidence data collated in the Nepal government's Bipad portal (<https://bipadportal.gov.np/>) from 13/05/2011 (the date of the first landslide record in the inventory) until the end of 2020, a period of 9.6 years. Data within the Bipad portal are compiled from reported landslide events, primarily sourced from the Nepal Police and local administrative officials (<https://bipadportal.gov.np/incidents/>). Importantly, the Bipad time series data excludes coseismic landslides from the 2015 Gorkha earthquake, which were not captured as part of the same landslide reporting system, but does include rainfall-triggered landslides before and after the earthquake. Landslide incidents are geolocated to (at least) an individual ward, which enables the impact attributes (fatalities, financial losses) to be aggregated to the same level. This inventory represents the best-available internally-consistent and national-scale record of landslide impacts in Nepal over this time period.

The realisation of exposure to landslides was assessed through comparison of ward-level modeled landslide susceptibility, population, and buildings, with recorded landslide fatalities and financial losses from Bipad. To consider broader patterns, kernel density estimates of ward-level summary values for modeled landslide susceptibility, population, population exposure and building exposure were calculated, and then re-run for only those wards that did and did not experience landslide incidents to identify any differences in locations with occurrence.

3. Results

3.1. Landslide Susceptibility

Our modeling shows that when considered in terms of the total land area covered by cells with a non-zero L_{suscept} value, 107,915 km² (77%) of Nepal is susceptible to landsliding to some degree. Notably, the distribution of susceptibility is heavily skewed toward lower values, with 46,038 km² (33%) of the land area having landslide susceptibility values >0 and <0.25 , and 61,878 km² (44%) being >0.25 (Figure 5). Only 7,196 km² (5%) of Nepal has a landslide susceptibility >0.5 , decreasing to just 90 km² ($<1\%$) for susceptibility values >0.75 .

The spatial distribution of susceptibility is highly non-uniform across Nepal, with a clear increasing trend northward as the relief increases in areas above c. 3,000 m elevation (Figure 1a; Figure 3a). Significantly, low to moderate landslide susceptibility is pervasive in the Middle Hills zone encompassing a large portion of Nepal. Landslide susceptibility in the lowland Terai region south of the Siwalik Hills is predominately low or negligible due to the relative lack of steep slopes (Figure 3a).

The 10 districts with the highest mean landslide susceptibility are within the High Himalayan region, broadly contiguous with the northern border with Tibet (Figure S5 in Supporting Information S1). The district of Manang has the highest mean landslide susceptibility (0.37), but Dolpa has the highest sum of susceptibility cell values (340,358) (Table S2 in Supporting Information S1). Nine of the 10 highest mean susceptibility wards are clustered

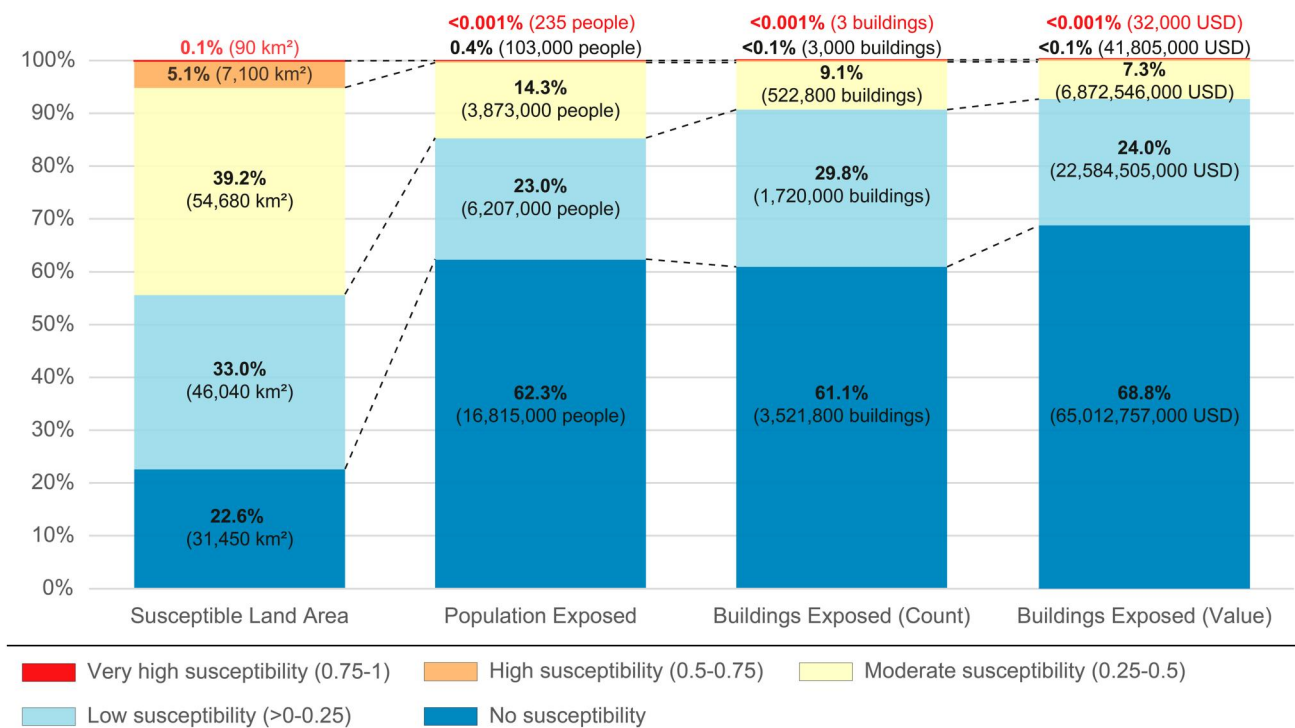


Figure 5. Comparison of the proportion of the land area of Nepal in different quartiles of landslide susceptibility with the proportion of the population and building stock count and value in those areas.

within three neighboring districts in the High Himalaya of western-central Nepal (Manang, Dolpa and Mustang), with the other located within Bajhang, another high mountain district in the far west (Figure S6; Tables S3 and S4 in Supporting Information S1). In total, five wards of northern Nepal are characterized by a mean landslide susceptibility >0.4 , with a further 311 having susceptibility ≥ 0.3 . Spatial variability in landslide susceptibility is also clearly present at the local (sub-district) scale, reflecting localized differences in the topographic variables used within the model (Figure 4a).

3.2. Population Exposure

The total population of Nepal in 2011 was 27 million, with the most populated areas being concentrated in two broad west-east zones coinciding with (a) the Middle Hills, and (b) the lowland Terai region to the south (Figure 3b). The Kathmandu Valley in central Nepal is the most densely populated area, with >2.5 million people estimated to be living in the contiguous districts of Kathmandu, Lalitpur and Bhaktapur. Beyond these areas, the population is largely dispersed in small settlements across rural areas (Rusk et al., 2022).

Of the total population of Nepal, at this scale of analysis, 10.2 million people (38% of the population) are located in areas of non-zero landslide susceptibility and hence are considered potentially exposed to landslides (Figure 5). Of this subset population (6.2 million; equivalent to 23% of the overall population) are in areas with low landslide susceptibility (first quartile, with $L_{\text{suscept}} < 0.25$). Population exposure is heavily skewed to low values, with 103,000 people ($<1\%$) in areas with susceptibility >0.5 , and 235 people in areas with susceptibility >0.75 (Figure 5). This indicates that whilst a considerable proportion of the population is to some degree exposed to landslides, the highest levels of exposure are faced by only a minority.

Population exposure to landslides is highest in the Middle Hill regions of Nepal, where there is typically a coincidence of moderately high landslide susceptibility and moderate to high population density (Figure 3c). Kavrepalanchok, Baglung, Dhading and Gulmi are the districts with the highest level of population exposure to landslides. However, within this broad zone of high exposure there is also pronounced variability, with notably high exposure peripheral to Kathmandu and Pokhara, Nepal's two largest cities, and in Syangja, Gulmi, Baglung and Parbat districts all clustered south-west of Pokhara (Figure 3c; Figure 1a). In other locations within the

Middle Hills, exposure to landslides is markedly lower where landslide susceptibility is moderately high but there is only limited coincidence with population.

Away from the Middle Hills, population exposure to landslides is generally lower (Figure 3c). In the High Himalaya, whilst landslide susceptibility is high, the population density is low, resulting in generally lower levels of exposure. The exceptions here are the major arterial road corridors linking Nepal to China that traverse high relief topography and attract peripheral development (Lennartz, 2013), such as the Arniko highway in Sindhu-palchok and the Kathmandu-Rasuwegadhi highway through Rasuwa (Figure 1a; Figure 3c; Figure 4), and proximal to significant infrastructure such as hydropower. Population exposure in the Terai is also typically low as a result of very low landslide susceptibility, despite high population densities.

Of the 20 most populous districts, only Kathmandu ranks in the 20 highest districts in terms of exposure to landslides (Figure S5; Table S2 in Supporting Information S1). Similarly, of the 20 districts with the highest mean landslide susceptibility, only three are ranked within the 20 highest in terms of population exposure (Sindhu-palchok, Gorkha and Bajhang). When analyzed at ward level, there is no overlap between the 10 highest wards for landslide susceptibility (mean or sum) and equivalent rankings for either population or population exposure (Figure S6; Tables S5 and S6 in Supporting Information S1). This demonstrates that exposure to landslides cannot be predicted on the basis of only landslide susceptibility or population (Figure S7 in Supporting Information S1). Based on a 90 m point grid distributed across the entire country, correlation between population and population exposure to landsliding is high ($R^2 = 0.91$), indicating that for those areas where there is potential for experiencing landslides, exposure increases if more people are present (Figure S7 in Supporting Information S1). Conversely, the correlation between landslide susceptibility and population exposure to landsliding is much lower ($R^2 = 0.16$), suggesting that higher susceptibility areas are typically not more populous. The distributions indicate that population exposure to landslides is most frequently coincident with moderately highly populated areas (e.g., the higher susceptibility periphery of otherwise low susceptibility settlements, or peri-urban developments), but not necessarily the densest population centers. Similarly, the majority of those exposed live within areas of moderate landslide susceptibility, but not typically in the most susceptible locations (Figure S7 in Supporting Information S1).

3.3. Building Exposure

High densities of buildings are concentrated within the cities of Kathmandu and Pokhara (Figure 3d), with much of the rest of Nepal having markedly lower building counts interspersed with small-scale nucleated settlements in which the building count is moderately high. In total, there were 5.8 million buildings recorded across the country, with 39% (2.2 million buildings) located within areas of non-zero landslide susceptibility (Figure 5). In contrast, 29.8% (1.7 million) are within the lowest quartile of landslide susceptibility ($0 < L_{\text{suscept}} < 0.25$), and 9.1% (526,000) are in areas with susceptibility > 0.25 . Only 2963 buildings (0.05%) are within areas 0.5 susceptibility, with only three of these being within areas with > 0.75 susceptibility.

The distribution of building exposure to landsliding (Figure 3e) differs considerably from that for the overall distribution of building count (Figure 3d), with building exposure being far more spatially heterogeneous. The pattern of building count exposure is again broadly situated throughout the Middle Hills, and with particularly high exposure around the Kathmandu Valley and Pokhara in Kaski district, but also in larger concentrations of contiguous districts in Western Nepal (e.g., Achham and Doti), Central-Western Nepal (e.g., Rolpa) and Eastern Nepal (e.g., Ilam, Bhojpur and Khotang).

High building stock values are also broadly concentrated within the central Nepal Middle Hills, and especially within the cities of Kathmandu, Pokhara and Bharatpur (Figure 3f), but also throughout much of the densely populated Terai to the south and certain districts in Western Nepal (e.g., Achham and Doti). Elsewhere in Nepal, estimated building values are generally lower, likely reflecting regional differences in vernacular construction and availability and affordability of building materials, but with localized concentrations of higher values concentrated within nucleated peri-urban settlements. The building stock value of Nepal totaled c. 94.5 billion USD, of which 31.2% (29.5 billion USD) is sited within areas of non-zero landslide susceptibility (Figure 5). The distribution of exposed buildings by susceptibility mirrors the population exposure, with a pronounced skew toward lower susceptibility values. In total, 24% (22.6 billion USD) of exposed building value is within areas with the lowest quartile of landslide susceptibility ($0 < L_{\text{suscept}} < 0.25$), while 7.3% (6.9 billion USD) is in areas with

susceptibility >0.25. Only 41.8 million USD (0.04%) of the national building stock value is within areas with >0.5 susceptibility, and 32,000 USD (<0.001%) is within areas with >0.75 susceptibility (Figure 5).

The distribution of building value exposure to landsliding (Figure 3g) broadly mirrors that for building value (Figure 3f), with the highest values again concentrated in the Middle Hills. High building value exposure is particularly skewed towards the periphery of cities such as Kathmandu, Pokhara and Bharatpur, reflecting the coincidence of very high building values and increasing landslide susceptibility away from the centre of the urban core. Away from the main cities, building value exposure is again high within discrete regions that have high building count exposure (Figure 3e), indicating the intersection of relatively high numbers of moderate-high value buildings and areas that are susceptible to landsliding. Outside of the Middle Hills building exposure to landslides is markedly lower, with negligible exposure for the high-value areas of the Terai (Figure 3g). Although landslide susceptibility in the High Himalaya to the north of the country is much higher, building exposure here is overall low, reflecting the low population numbers and low aggregate building values (Figure 3). These broad spatial trends in building value and exposure contain considerable localised variability, resulting from intra-settlement differences in building size, construction type and exposure to landsliding (Figure 4).

Of the 20 highest ranked districts in terms of total building count, 16 are ranked within the 20 highest districts for population count and 16 are also ranked within the 20 highest districts for building value (Table S2 in Supporting Information S1). However, only four of the 20 highest ranked building count districts are within the 20 highest districts for building count exposure, and none are within the top 20 ranked districts for either landslide susceptibility metric (Table S2 in Supporting Information S1). The building value results also reflect this, with only five of the 20 highest ranked districts for building value also being within the top 20 ranked districts for building value exposure, and only one being within the top 20 for landslide susceptibility (Table S2 in Supporting Information S1). The ward summaries also reflect this broad pattern, with generally good correspondence between the rankings for ward-level building count and building value, but lower correspondence between these and associated exposure variables or landslide susceptibility (Tables S7–S10 in Supporting Information S1). This reflects the marked differences in the distributions of ward-level building counts and values when compared with the distribution of landslide susceptibility (Figure S6 in Supporting Information S1).

The correlation between cellwise building count and building count exposure is high ($R^2 = 0.82$), indicating that, where a potential landslide hazard exists, building exposure is greater if the number of buildings present is higher, which is as expected given the aggregated nature of this variable (Figure S7 in Supporting Information S1). The same situation is present with building value, which has a high correlation with building value exposure ($R^2 = 0.87$). However, the equivalent correlations are much lower between both building count exposure and landslide susceptibility ($R^2 = 0.38$), and building value exposure and landslide susceptibility ($R^2 = 0.27$), which shows that locations with higher building exposure are not simply a result of the level of landslide susceptibility. The majority of building value exposure arises in moderately high landslide susceptibility areas coincident with relatively low building values. Only low-moderate positive correlations exist between cellwise population count and building count exposure ($R^2 = 0.14$), and between population count and building value exposure ($R^2 = 0.31$) (Figure S7 in Supporting Information S1).

3.4. Landslide Exposure and Impact

In total, there were 2,120 landslides recorded in the Bipad platform between 13/05/2011 and 31/12/2020. Within these records there were 403 landslides (19%) recorded for the c. four years prior to the 2015 Gorkha earthquake, and 1,717 landslides (81%) for the c. 5.7 years after the earthquake. These landslides led to an estimated 1,205 fatalities, 996 injuries, the loss of 2,977 livestock, and the destruction of 2,765 buildings. The combined economic cost of these events was >1.7 billion Nepali rupees (~\$14.3 million USD).

Landslides were recorded within 861 different wards (13% of the total) distributed across Nepal, although most of these wards (596; 66%) experienced only one landslide incident (Figure 6a). Very few wards recorded higher numbers of landslides, with 69 wards (8%) recording ≥ 5 incidents, 39 wards (4.5%) with ≥ 10 incidents, and only 18 wards (2%) with ≥ 20 incidents. Wards impacted by landslides were generally concentrated within the Middle Hills region but there are additional clusters further north, especially north-central and north-eastern Nepal. In general terms, the wards impacted by a higher number of landslides were focused in the High Himalaya region,

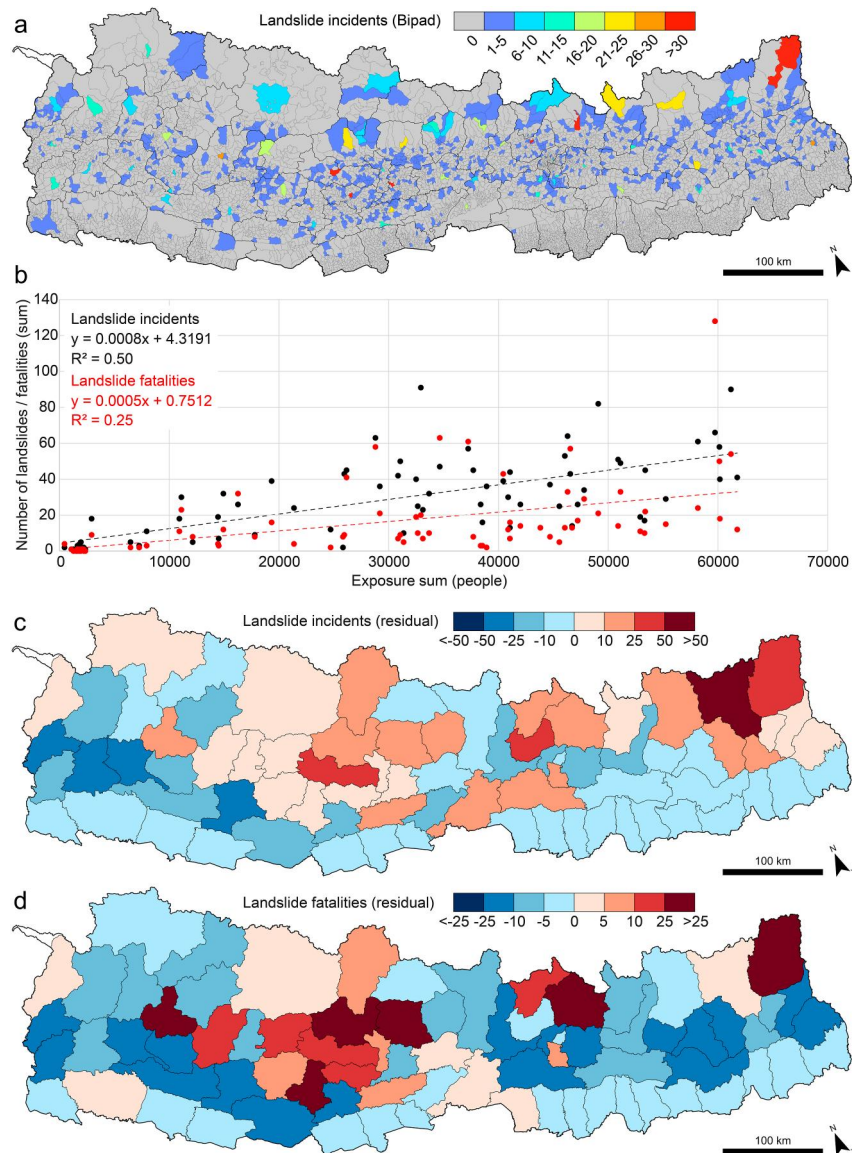


Figure 6. Realisation of landslide risk, displayed as (a) the number of documented landslide incidents occurring in each ward during the period 13/05/2011 and 31/12/2020 (data from bipadportal.gov.np); (b) correlation between the district-wise total number of landslide incidents (black dots) and fatalities (red dots) and the district-wise sum of population exposure; (c) the district-level residual between the predicted number of landslide incidents, based on the regression equation in (b), and the actual recorded number of incidents; and (d) the corresponding district-level residuals for landslide fatalities. In both (c) and (d), red colors indicate that more landslides or landslide-related fatalities occurred than would be expected from the regression equations, and blue colors indicate that there were less than would be expected.

although it should be noted that as wards are intended to encompass an approximately equal electorate, those in more remote locations often cover a much larger geographical extent.

Moderate positive correlations exist between population exposure and the number of landslide incidents ($R^2 = 0.5$) and landslide-related fatalities ($R^2 = 0.25$) when the data are aggregated at district level (Figure 6b). Assuming that the Bipad loss data are sufficiently complete to represent long-term rates and patterns of landslide impacts, the analysis of the spatial distribution of residuals from the linear regressions shown in Figure 6b indicates that some areas of Nepal have experienced proportionately more landslides and landslide-related fatalities than the population exposure model would suggest, whilst other areas have experienced less (Figures 6c and 6d). Districts experiencing more reported landslide incidents than expected are clustered in the northeast, in the higher

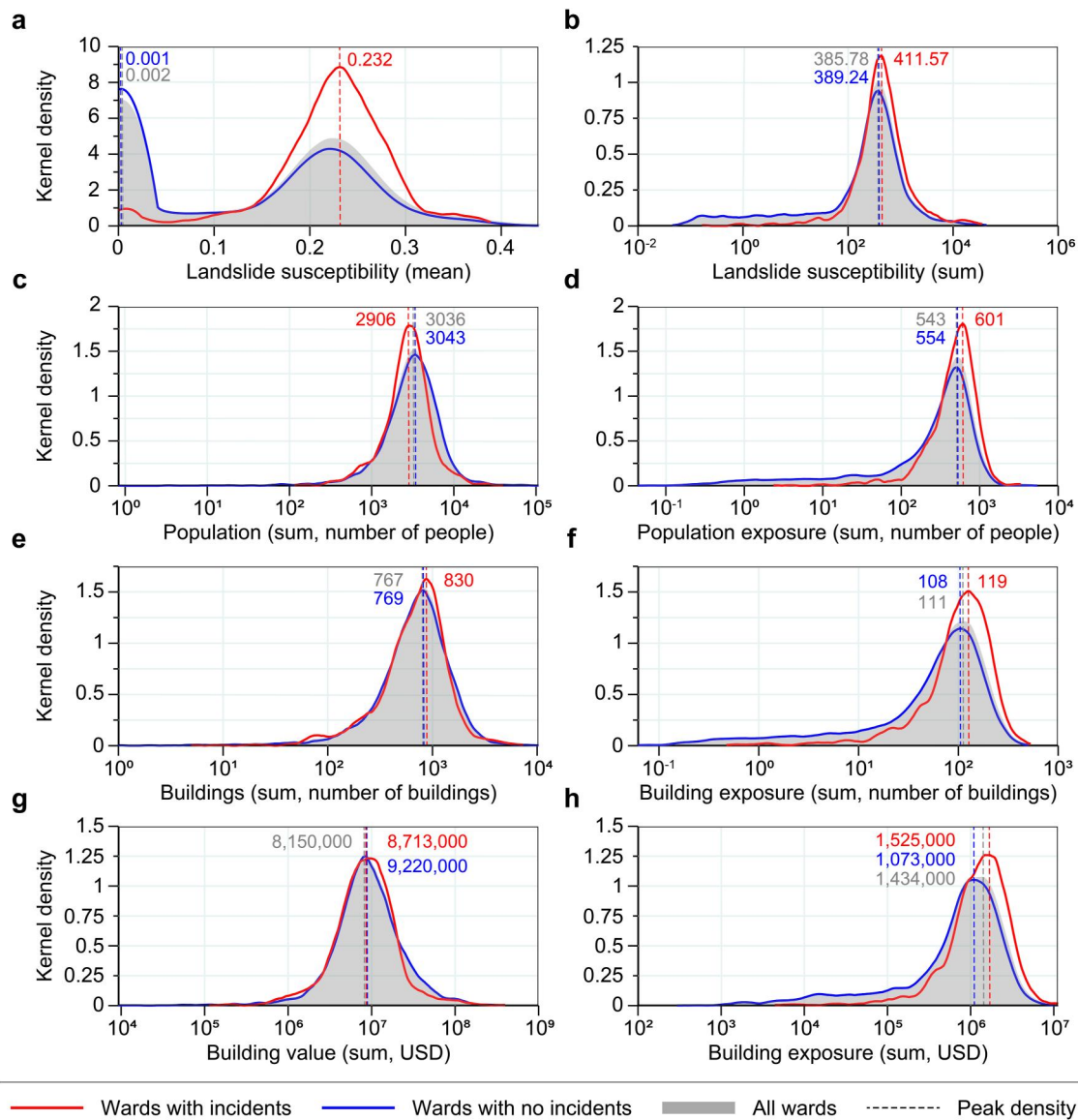


Figure 7. Kernel density distributions of ward-level (a) mean landslide susceptibility, (b) total landslide susceptibility (sum), (c) population count, (d) population exposure, (e) building count, (f) building count exposure, (g) building value, and (h) building value exposure. In each case, separate density curves have been plotted for wards where landslide incidents were recorded on Bipad (red), and those with no recorded landslides (blue), as well as for all wards combined (gray). Dashed lines show the mode of each distribution.

relief districts in northern central Nepal, and in the Siwalik Hills further south (Figure 6c). Districts with fewer reported landslides are clustered within the Middle Hills region of western Nepal. The pattern of residuals for landslide fatalities is broadly similar but with an additional cluster of severely-impacted districts within the Middle Mountains and Middle Hills region of central-western Nepal (Figure 6d).

In contrast, no significant correlations exist when the number of landslide incidents within each administrative ward is compared to either landslide susceptibility or population exposure. There are, however, notable differences between the kernel density distributions based on all wards that did record landslide incidents and those that did not (Figure 7). The density distributions for wards that did record landslides are typically shifted toward higher landslide susceptibility values (mean and sum), with a noticeable lack of wards experiencing landslides in low susceptibility areas (Figures 7a and 7b). Although wards where reported landslide incidents did occur typically have lower populations and lower overall building values (Figures 7c and 7e), they also typically record higher population exposure and building exposure values (Figures 7d and 7f).

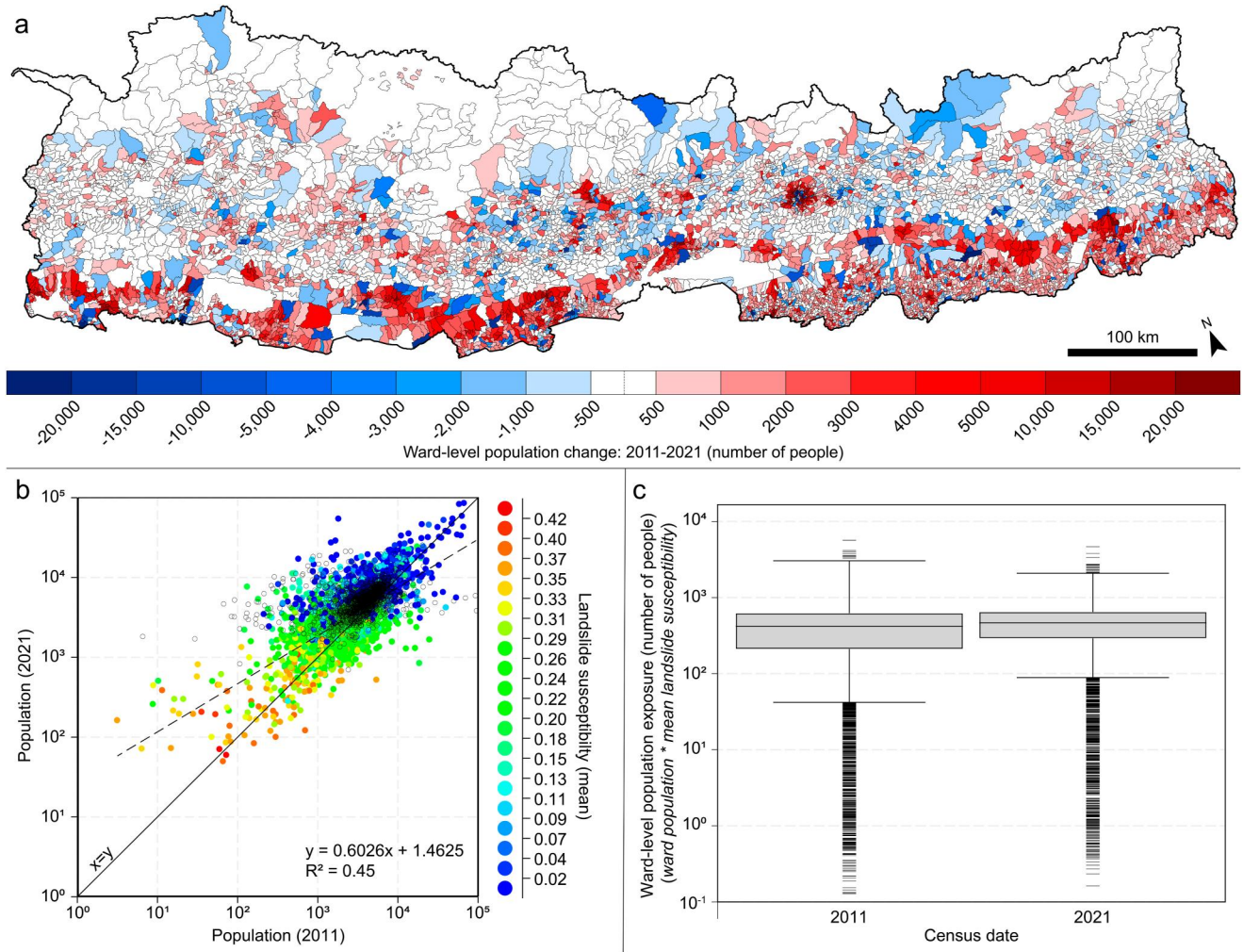


Figure 8. (a) Map of Nepal showing ward-level population change between 2011 and 2021, with population growth indicated by red colors and population decline indicated by blue colors. (b) Scatter plot showing the correlation between the 2011 and 2021 population counts for each ward within Nepal. Individual points are colored by the mean landslide susceptibility value for that particular ward, with reds representing high susceptibility and blues low susceptibility. The solid line represents the 1:1 line and the dashed line indicates the linear fit through all ward points ($R^2 = 0.45$). (c) Box plots showing the distribution of population exposure to landsliding across all wards in Nepal for 2011 and 2021. Since the population data for 2021 is only available as ward-level totals, population exposure here has been calculated as the mean landslide susceptibility for each ward, multiplied by the corresponding population for each year.

3.5. Temporal Variability in Landslide Exposure

According to the preliminary census results, the population of Nepal increased from 27 million in 2011 to 29 million in 2021, an overall increase of $>7\%$. Most wards (66%) experienced an increase in population during this 10-year period, with particular concentrations of higher population increases in the Terai to the south of the country, around the urban centers of Kathmandu and Pokhara, and in clusters distributed throughout the Middle Hills (Figure 8a). Interspersed amongst this were clusters of wards that experienced population decline, especially within the Middle Hills and further north into the High Himalaya.

There is a moderate correlation ($R^2 = 0.45$) between the ward-level population in 2011 and the equivalent population in 2021 (Figure 8b). These results show that the mean landslide susceptibility for wards with lower populations is generally higher than in wards with higher populations (Figure 8b), which mirrors the broader distribution of population exposure described above (Section 3.2). Wards with higher mean landslide susceptibilities do not show a single trajectory in terms of population change, instead exhibiting considerable variability and with some wards experiencing a population decline but others showing a notable population increase (Figure 8b).

In the absence of high-resolution population data comparable to the 90 m WorldPop data from 2011, the change in population exposure to landslides between 2011 and 2021 was assessed by multiplying ward-level mean landslide susceptibility by the equivalent total ward population for each year (Figure 8c). The increase in population between these dates resulted in an overall increase in population exposure to landsliding, with a mean of 329 exposed people per ward in 2011 and 355 in 2021 (median values = 274 and 350 respectively). However, the spatial variability in population change meant that this increase was not uniform across the country, with an upward shift in the average ward-level exposure distribution, but also a notable contraction in the overall spread of exposure values (Figure 8c).

4. Discussion

4.1. Scale and Resolution

Despite being a global landslide hotspot (Emberson et al., 2020) and experiencing significant landslide impacts annually (Froude & Petley, 2018), efforts to systematically assess and reduce landslide hazard and risk across Nepal remain fragmentary (ICIMOD, 2016; Meena et al., 2021). As a result, the distribution and concentration of exposure to landslides has remained largely anecdotal and has most often been described only in general terms, lacking focus on the scale and precise nature of the problem. Consequently, a precautionary approach has assumed that exposure to landslides is high and homogenous, as has been the case for earthquake hazard (e.g., Stein et al., 2018). However, it is well-established from Nepal and elsewhere that landslide hazard and exposure, and hence risk, can vary from negligible to extreme over short (10s of m) distances (Milledge et al., 2019; Wymann von Dach et al., 2017).

We have presented a spatially consistent model of landslide susceptibility and exposure, comparable with similar synoptic evaluations conducted elsewhere (e.g., Depicker et al., 2021). The fuzzy logic-based approach allows for the inconsistencies otherwise introduced by low resolution and often spatially inconsistent covariate data to be overcome (Reichenbach et al., 2018). The model can reproduce the broad pattern of landslide occurrence, at least to the extent that it is visible in the best available national-scale inventory, albeit with some important differences that we explore below. Fundamentally, the model identifies that exposure to landslides is not ubiquitous in Nepal, but conversely does show that many wards include specific locations at moderate to high landslide susceptibility levels.

As the scale of landslide susceptibility analysis increases, it is often necessary to reduce resolution for computational reasons (Chang et al., 2019), yet the impacts of landslides that accrue the greatest total losses in Nepal are experienced very much at the level of individual households (Sidle et al., 2017; Sudmeier-Rieux et al., 2012). It is also common that large-scale landslide models, tuned to large geographical areas, can saturate and provide little discernible granularity within higher risk areas (e.g., Nadim et al., 2006), and so can therefore be of limited utility on the ground (Brock et al., 2020; Chang et al., 2019). Both of these effects are problematic for identifying the areas that are of greatest societal concern for reducing landslide losses. The analysis presented here retains the high spatial resolution (90 m) necessary to evaluate local exposure to landslides, but does so at a national scale. Importantly, the modeling approach only defines a relative indicator of susceptibility and exposure, identifying the most likely location to experience a landslide, and scoring all other locations relative to this. As such, this approach does not replace the need for on-the-ground site assessments of slope stability, but does add clarity to decisions around where such investigations are likely to be needed.

4.2. Patterns of Susceptibility and Exposure

It is clear from our analysis that the footprints of landslide susceptibility and population differ considerably, and neither independently provides an adequate proxy for population exposure to landsliding (Figures 3 and 4), mirroring patterns of susceptibility and population observed at larger scale across the Himalaya (e.g., Rusk et al., 2022). Landslide susceptibility is highest in the High Himalaya, where extreme slopes and relief generate conditions highly favorable to instability (Figure 3a). Susceptibility remains at moderately high levels in many locations across the Middle Hills, but even at this resolution (90 m) it is far from uniform. Conversely, whilst population densities are in general low in the High Himalaya, the Middle Hills have a moderately high density dispersed rural population, interspersed by notable often small urban centers and transport corridors (Figures 3b, 3d and 3f). This intersection of susceptibility and population produces the concentration of exposure to landslides running through the Middle Hills (Figures 3c, 3e and 3g). Even this broad band of apparently concentrated exposure, however, is highly heterogenous. The highest susceptibility areas (the 0.1% of the country with

$L_{\text{suscept}} > 0.75$) are (a) dispersed across the Middle Hills, but (b) locally manifest as a specific coincidence of housing and landslides, providing a clear geographical basis for prioritization of efforts for reducing losses or for assessing case-loads of people exposed to landslides. Importantly, such concentrations do not typically reflect a ubiquitous high susceptibility overlaying pockets of population, but rather the product of a complex distribution of moderate rural population density and a similar distribution of moderate levels of landslide susceptibility.

4.3. Implications for Mitigation and Case-Loads

We demonstrate that most Nepalis who reside in areas at a non-zero level of exposure to landslides are within locations classified as low susceptibility (6.2 M, $L_{\text{suscept}} < 0.25$), but concerning a significant minority reside in areas with moderate or higher levels of susceptibility (103,000, $L_{\text{suscept}} > 0.5$) (Figure 5). Whilst a susceptibility model only provides a probabilistic assessment of where hazards are most likely to occur, and not who will be impacted by the next landslide, these numbers importantly provide clarity around the scale of total landslide risk faced at a national level, and indicate where mitigation efforts could be focused. Politically, this approach defines a more tangible and perhaps manageable case-load to prioritize disaster risk reduction and contingency planning at national level, but also for individual municipalities which hold much of the responsibility for mitigation (Oven et al., 2021).

Our analysis also demonstrates that 39% of all buildings in Nepal and 31% of the monetary value of the building stock is exposed to a non-zero landslide susceptibility (Figure 5). This exposure exhibits a pronounced skew to lower values, with <0.001% of building value in areas of highest landslide susceptibility ($L_{\text{suscept}} > 0.75$), representing <\$32,000 of total built asset value and so a very small number of houses. We note a subtle but apparent difference between the distribution of exposure by building count (Figure 3e) and building value (Figure 3g), whereby exposure by number is more spatially uniform and exposure by value shows more locations with higher degrees of exposed building value. This suggests a spatially pervasive experience of landsliding across this region of Nepal. This demonstrates that the majority rural population of Nepal can experience moderate to high degrees of exposure to landslides, reaffirming the fact that landsliding in Nepal remains primarily a concern for rural communities (Aksha et al., 2019).

Importantly, our results also indicate a stark sensitivity of landslide exposure to changes in population density and distribution, which is of particular significance given recent and projected patterns of urbanization throughout Nepal and the Himalayan region more broadly (Chen et al., 2023). Although no population data are yet available at the same resolution that we have used for our detailed analysis of spatial differences in exposure, ward-level assessment of population change between 2011 and 2021 indicates both an overall increase in population exposure to landsliding and spatial variability in the trajectory of exposure change through time (Figure 8). Worryingly, our modeling also tentatively suggests a sensitivity of landslide exposure in Nepal to even a minor uplift in landslide hazard (susceptibility). For example, a +5% increase in landslide susceptibility, which could plausibly occur through projected increases in the magnitude and frequency of intense rainfall events, would expand areas where $L_{\text{suscept}} > 0.5$ to include an additional c. 55,000 people, an increase of 53% over the results shown in Figure 5, even with no corresponding change in population. Taken together, these results clearly demonstrate the complex interplay between the spatially and temporally variable nature of landslide hazard and population exposure, which together form interconnected but dynamic components of landslide risk. In Nepal, this means that exposure to landslides is increasingly likely to be part of everyday life in the densely populated Middle Hills, and reinforces the need to find effective and sustainable ways of living safely alongside landslides going forward.

4.4. Comparison With Landslide Impacts and Implications for Risk Assessment

The generation of an empirically based landslide exposure model enables a comparison to landslide impact data. At the macro level, we observe that c. 100,000 people reside in areas considered at moderate to high landslide risk in Nepal, yet c. 200 people are killed by landslides each year on average (Petley et al., 2007). Despite the focus brought by our analysis in locating those most at risk, there is still considerable effort needed to identify how exposure to landslides translates into impact and loss in the short term. At a broad scale, the geographical pattern of losses from the landslide inventory in Bipad maps onto areas modeled as at higher population exposure when aggregated to district level (Figure 6). Over the approximately 10-year duration of this archive, however, general patterns can be distorted by the presence or absence of single large events, or insufficient numbers of small events in locations where they are possible, meaning that aggregation to larger geographical areas is needed. Whilst the

variable size of administrative areas makes direct comparison difficult, we observe that some districts have experienced higher or lower landslide impacts than expected. For example, we observe a set of districts that extend into the High Himalaya, with a significant number of landslides and landslide-related fatalities, and with high landslide susceptibility but only low to moderate concentrations of people (Figures 6c and 6d). This demonstrates that high landslide risk can and does extend beyond those areas where impacts are most frequently experienced and reported, and particularly into areas with high susceptibility in the High Himalaya.

This pattern also highlights the potential for catastrophic impacts in high mountain regions, similar to recent events in Uttarakhand (Ziegler et al., 2014), Chamoli (Shugar et al., 2021), and Melamchi (Maharjan et al., 2021), which vividly demonstrate the potential consequences of people being located in highly exposed places, such as immediately below unstable slopes, or adjacent to channels that experience debris flows. Two important implications arise: first, where there is pressure for development in and through these high mountain regions, commonly associated with transboundary transport links (Hearn & Shakya, 2017; Sudmeier-Rieux et al., 2019) or the proliferation of Himalayan hydroelectric power (Schwanghart et al., 2018), great care is needed to minimize landslide risk by reducing exposure where possible and ensuring that already high levels of landslide hazard are not further increased. Second, it is important to remember that the patchy agreement between the population exposure model and landslide fatalities in the High Himalaya visible in Figure 6 may be due to the short historical record of events and the changing pattern of settlement in these areas. In other words, the lack of high exposure may not be a good indication of future safety, especially in areas where development is only recently drawing more people to the region. Thus, there may be latent landslide risk that has not yet been realized. This is particularly the case in high-elevation areas with widespread high landslide susceptibility and where development is only relatively recently drawing more people to these regions (Wester et al., 2019). Similar areas of high modeled susceptibility but with low observed historical impacts are also of concern, and may reflect a latent landslide risk. The concern here is not just one of a higher degree of hazard or likelihood because an event has not *yet* occurred, but more that the risks are high but recognition may be limited because of few incidents in living memory, and that assessments of risk based on impacts will systematically underrepresent risks in these areas.

4.5. Future Developments and Refinements

Inevitably a modeling exercise such as that described here includes assumptions and limitations. The model can only be as good as the input data, and the exposure to landslides assessed here remains sensitive to the inventory upon which it is trained. It is important to emphasize that the training data here are limited to rainfall-triggered landslides from 14 districts in central Nepal. Despite this geographical limitation, the high AUROC value shows that the fuzzy modeling approach provides a reasonable first-order indication of landslide susceptibility within the training area (Figure S4 in Supporting Information S1), and our analysis of topographic input variables shows that covariate distributions within the training area are largely representative of the whole of Nepal (Figure S2 in Supporting Information S1). As argued for in other regions of high landslide risk (e.g., the East African Rift (Monsieurs et al., 2018)), there is a clear need for up-to-date mapping of landslides at a national scale, and particularly across the populous Middle Hills and Siwaliks of Nepal, to underpin improvements in modeling risk in the future. Over short time scales the model cannot reflect the often highly localized effects of triggers such as cloud burst events, where the local scale variability of susceptibility may be overprinted by the footprint of the triggering event. By including full mapped landslide footprints, we also conflate landslide source and debris, and so our model predicts the susceptibility of being *within* a landslide, rather than at the point of failure or runout specifically. In this sense, and advantageously, the model takes a precautionary approach appropriate to the context. Further, and importantly, Nepal remains one of the world's landslide hotspots, and so the discretization presented here likely describes a spectrum focused upon the higher end of global levels of landslide risk: critically, a landslide could still happen across much of Nepal where topography allows. As such, the primary purpose of these data is in defining relative exposure to landslides, and using this to inform preparedness and planning. Critically, to enable this analysis to move toward an appraisal of *risk*, household level data on vulnerability to landslides is needed, but currently remains absent.

Comparison of the results with landslide impacts also depends critically on the availability of consistent, reliable and widespread impact data. In Nepal, recent efforts to institutionalize the systematic capture of hazard impact data have made progress (Neupane, 2020), and offer some insight into the nature of landslide impacts (Adhikari & Tian, 2021). However, these records remain temporally short, have low spatial resolution (e.g., ward or municipal level location information at best), and are inevitably associated with only observed impactful events rather than

all landslides (Stanley & Kirschbaum, 2017). They therefore need careful treatment when used for assessing future risk (Huggel et al., 2015).

5. Conclusions

We have presented a nationwide landslide susceptibility model for Nepal, based upon mapped landslide training data modeled using a fuzzy overlay approach. We have overlaid this with data describing population and building location to explore the spatial pattern of exposure to landslides. Whilst our results broadly mirror patterns seen in the available record of landslide impact data, here we add considerable granularity to where, and therefore who, faces potential landslide hazards. We draw the following conclusions from our analysis:

- A full picture of exposure to landslides in Nepal can at present only be derived from the overlay of landslide susceptibility and population or building data, with each of these independently unable to fully explain the pattern of landslide risk. Exposure to landslides emerges from the intersection of spatially variable susceptibility and a dispersed largely rural population, and thus varies over very short distances.
- Landslide susceptibility is highest in the High Himalaya, but this only exposes people in isolated pockets in this otherwise sparsely inhabited region. Exposure to landslides in the High Himalaya, where present, is however likely to be high and will likely increase with further development, such as that associated with the growth of hydropower.
- Based upon 2011 population data, over 100,000 people are living in areas deemed to be at moderate to high levels of exposure to landslides. Most of these live in the Middle Hill districts where landslide exposure is most concentrated. Importantly, even across this region exposure is highly variable, with the majority of land, buildings and people facing relatively negligible or low levels of exposure.
- The analysis presented identifies the locations across Nepal that are at a relatively high level of exposure to landslides, and so provides a first-order estimate of the scale and geography of the challenge faced in reducing landslide risk in Nepal from national to local administrative levels.
- Exposure to landslides appears insensitive to building value, and reflects that the precise house location in rural areas is commonly a trade-off between livelihood opportunities and environmental risks. As a result, high value houses may at times be found in locations with higher landslide susceptibility, conflating a simple association between wealth/poverty and exposure to landslides.
- Critically, a comparison of this model with landslide impact archives suggests that, while the broad outlines of those impacts are captured by the model, the available impact records may be too short to fully understand future landslide risks. Our analysis thus shows a pressing need for greater attention to be placed on the collation and maintenance of baseline data on landslides and their impacts, such as a nationwide landslide inventory, which is essential for: identifying the root causes of landslide risk, notably those associated with variations in vulnerability not described here; shaping future policy and practice; and fully understanding the future impacts of climate change on landsliding.
- Our modeling results indicate a high degree of sensitivity of the case load of people exposed to landslides to both future changes in population density and distribution, and to changes in landslide susceptibility: a +5% increase in susceptibility will place an additional 55,000 (+53%) people into the moderate class of exposure to landslides.

Data Availability Statement

The landslide susceptibility model on which the analysis within this article is based is available in Kinsey et al. (2023). This landslide susceptibility model and related administrative-level summaries are also available for viewing on the Bipad disaster information management system (<https://bipadportal.gov.np/risk-info/#/hazard>). Population data are openly available from WorldPop (2020), and the building exposure data are freely accessible from the METEOR Project Consortium (2020). The ward-level 2021 census data are available from the Government of Nepal's National Statistics Office (Government of Nepal, 2023).

References

- Adhikari, B. R., & Tian, B. (2021). Spatiotemporal distribution of landslides in Nepal. In *Handbook of disaster risk reduction for resilience* (pp. 453–471). Springer.
- Aksha, S. K., Juran, L., Resler, L. M., & Zhang, Y. (2019). An analysis of social vulnerability to natural hazards in Nepal using a modified social vulnerability index. *International Journal of Disaster Risk Science*, 10(1), 103–116. <https://doi.org/10.1007/s13753-018-0192-7>

Acknowledgments

This research has been supported by the UKRI-DFID SHEAR program (201844-112), the EPSRC project “Risk at the Margins” (EP/T024747/1), the EU ECHO HIP project “Risk informed landslide management in Nepal’s hill areas” (ECHO/-XA/BUD/2020/91026), and by a grant from the Global Challenges Research Fund Multi-Hazard and Systemic Risk programme for the “Sajag-Nepal” project (NE/T01038X/1). We thank Dalia Kirschbaum and her team at NASA Goddard Space Flight Center for constructive discussions on landslide susceptibility modelling, and Kay Smith (BGS) and Charles Huyck (ImageCat) for their valuable input regarding the METEOR building data. We also thank S. N. Shrestha and G. Jimée (NSET-Nepal), and T. Sumner and S. Dugar (UK FCDO) for their time and advice in developing this work.

- Arouri, M., Nguyen, C., & Youssef, A. B. (2015). Natural disasters, household welfare, and resilience: Evidence from rural Vietnam. *World Development*, 70, 59–77. <https://doi.org/10.1016/j.worlddev.2014.12.017>
- Brock, J., Schratz, P., Petschko, H., Muenchow, J., Micu, M., & Brenning, A. (2020). The performance of landslide susceptibility models critically depends on the quality of digital elevation models. *Geomatics, Natural Hazards and Risk*, 11(1), 1075–1092. <https://doi.org/10.1080/19475705.2020.1776403>
- Bui, D. T., Pradhan, B., Lofman, O., Revhaug, I., & Dick, O. B. (2012). Spatial prediction of landslide hazards in Hoa Binh province (Vietnam): A comparative assessment of the efficacy of evidential belief functions and fuzzy logic models. *Catena*, 96, 28–40. <https://doi.org/10.1016/j.catena.2012.04.001>
- Carrara, A., Cardinali, M., Deti, R., Guzzetti, F., Pasqui, V., & Reichenbach, P. (1991). GIS techniques and statistical models in evaluating landslide hazard. *Earth Surface Processes and Landforms*, 16(5), 427–445. <https://doi.org/10.1002/esp.3290160505>
- Carrara, A., Cardinali, M., Guzzetti, F., & Reichenbach, P. (1995). GIS technology in mapping landslide hazard. In *Geographical information systems in assessing natural hazards* (pp. 135–175). Springer.
- Chang, K. T., Merghadi, A., Yunus, A. P., Pham, B. T., & Dou, J. (2019). Evaluating scale effects of topographic variables in landslide susceptibility models using GIS-based machine learning techniques. *Scientific Reports*, 9(1), 1–21. <https://doi.org/10.1038/s41598-019-48773-2>
- Chen, T. H. K., Pandey, B., & Seto, K. C. (2023). Detecting subpixel human settlements in mountains using deep learning: A case of the Hindu Kush Himalaya 1990–2020. *Remote Sensing of Environment*, 294, 113625. <https://doi.org/10.1016/j.rse.2023.113625>
- Cieslik, K., Shakya, P., Upreti, M., Dewulf, A., Russell, C., Clark, J., et al. (2019). Building resilience to chronic landslide hazard through citizen science. *Frontiers in Earth Science*, 7, 278. <https://doi.org/10.3389/feart.2019.00278>
- Corominas, J., van Westen, C. J., Frattini, P., Cascini, L., Malet, J. P., Fotopoulou, S., et al. (2014). Recommendations for quantitative landslide risk assessment. *Bulletin of Engineering Geology and the Environment*, 73(2), 209–263.
- Depicker, A., Jacobs, L., Mboga, N., Smets, B., Van Rompaey, A., Lennert, M., et al. (2021). Historical dynamics of landslide risk from population and forest-cover changes in the Kivu Rift. *Nature Sustainability*, 4(11), 965–974. <https://doi.org/10.1038/s41893-021-00757-9>
- Dilley, M., Chen, R. S., Deichmann, U., Lerner-Lam, A. L., & Arnold, M. (2005). *Natural disaster hotspots: A global risk analysis*. The World Bank. Retrieved from <https://openknowledge.worldbank.org/handle/10986/7376>
- Eckholm, E. P. (1975). The deterioration of mountain environments. *Science*, 189(4205), 764–770. <https://doi.org/10.1126/science.189.4205.764>
- Ehrlich, D., Melchiorri, M., & Capitani, C. (2021). Population trends and Urbanisation in mountain ranges of the world. *Land*, 10(3), 255. <https://doi.org/10.3390/land10030255>
- Embersson, R., Kirschbaum, D., & Stanley, T. (2020). New global characterisation of landslide exposure. *Natural Hazards and Earth System Sciences*, 20(12), 3413–3424. <https://doi.org/10.5194/nhess-20-3413-2020>
- Fleuchaus, P., Blum, P., Wilde, M., Terhorst, B., & Butscher, C. (2021). Retrospective evaluation of landslide susceptibility maps and review of validation practice. *Environmental Earth Sciences*, 80(15), 1–15. <https://doi.org/10.1007/s12665-021-09770-9>
- Froude, M. J., & Petley, D. N. (2018). Global fatal landslide occurrence from 2004 to 2016. *Natural Hazards and Earth System Sciences*, 18(8), 2161–2181. <https://doi.org/10.5194/nhess-18-2161-2018>
- Fuchs, S., Keiler, M., & Zischg, A. (2015). A spatiotemporal multi-hazard exposure assessment based on property data. *Natural Hazards and Earth System Sciences*, 15(9), 2127–2142. <https://doi.org/10.5194/nhess-15-2127-2015>
- Gaidzik, K., & Ramírez-Herrera, M. T. (2021). The importance of input data on landslide susceptibility mapping. *Scientific Reports*, 11(1), 1–14. <https://doi.org/10.1038/s41598-021-98830-y>
- Gentle, P., & Maraseni, T. N. (2012). Climate change, poverty and livelihoods: Adaptation practices by rural mountain communities in Nepal. *Environmental Science & Policy*, 21, 24–34. <https://doi.org/10.1016/j.envsci.2012.03.007>
- Gerrard, J., & Gardner, R. (2002). Relationships between landsliding and land use in the Likhu Khola drainage basin, Middle Hills, Nepal. *Mountain Research and Development*, 22(1), 48–55. [https://doi.org/10.1659/0276-4741\(2002\)022\[0048:rlalu\]2.0.co;2](https://doi.org/10.1659/0276-4741(2002)022[0048:rlalu]2.0.co;2)
- Glade, T., & Crozier, M. J. (2005). *The nature of landslide hazard impact. Landslide hazard and risk* (pp. 43–74). Wiley.
- Government of Nepal. (2023). National Statistics Office. National Population and Housing Census 2021: Ward Report [Dataset]. Government of Nepal. Retrieved from <https://censusnepal.cbs.gov.np/results/downloads/ward>
- Guzzetti, F., Reichenbach, P., Cardinali, M., Galli, M., & Ardizzone, F. (2005). Probabilistic landslide hazard assessment at the basin scale. *Geomorphology*, 72(1–4), 272–299. <https://doi.org/10.1016/j.geomorph.2005.06.002>
- Hearn, G. J., & Shakya, N. M. (2017). Engineering challenges for sustainable road access in the Himalayas. *The Quarterly Journal of Engineering Geology and Hydrogeology*, 50(1), 69–80. <https://doi.org/10.1144/qjegh2016-109>
- Huggel, C., Raissig, A., Rohrer, M., Romero, G., Diaz, A., & Salzmann, N. (2015). How useful and reliable are disaster databases in the context of climate and global change? A comparative case study analysis in Peru. *Natural Hazards and Earth System Sciences*, 15(3), 475–485. <https://doi.org/10.5194/nhess-15-475-2015>
- Huyck, C., Hu, Z., Amyx, P., Esquivias, G., Huyck, M., & Eguchi, M. (2019). METEOR: Exposure data classification, metadata, population and confidence assessment. Report number: M3.2/P. Retrieved from https://meteor-project.org/storage/METEOR_M3.2P_Exposure_Data_Classification_Metadata_Population_and_Confidence_Assessment.pdf
- ICIMOD. (2016). Consultation workshop on landslide inventory, risk assessment, and mitigation in Nepal. In *ICIMOD. Proceedings 2016/2. Kathmandu*. Retrieved from <https://lib.icimod.org/record/31875>
- Jakub, M. (2021). Landslides in a changing climate. In T. Davies, N. Rosser, & J. F. Shroder (Eds.), *Landslide hazards, risks, and disasters* (2nd ed.). Elsevier.
- Keiler, M. (2004). Development of the damage potential resulting from avalanche risk in the period 1950–2000, case study Galtür. *Natural Hazards and Earth System Sciences*, 4(2), 249–256. <https://doi.org/10.5194/nhess-4-249-2004>
- Khanal, K., Budhathoki, N. R., & Erbstein, N. (2019). Filling OpenStreetMap data gaps in rural Nepal: A digital youth internship and leadership programme. *Open Geospatial Data, Software and Standards*, 4(1), 12. <https://doi.org/10.1186/s40965-019-0071-1>
- Kincey, M., Rosser, N., Swirad, Z., Robinson, T., Shrestha, R., Singh-Pujara, D., et al. (2023). National-scale rainfall-triggered landslide susceptibility and exposure in Nepal (Version 1) [Dataset]. Zenodo. <https://zenodo.org/record/8307964>
- Kincey, M. E., Rosser, N. J., Robinson, T. R., Densmore, A. L., Shrestha, R., Pujara, D. S., et al. (2021). Evolution of coseismic and post-seismic landsliding after the 2015 Mw 7.8 Gorkha earthquake, Nepal. *Journal of Geophysical Research: Earth Surface*, 126(3). <https://doi.org/10.1029/2020jf005803>
- Kirschbaum, D. B., Adler, R., Hong, Y., Hill, S., & Lerner-Lam, A. (2010). A global landslide catalog for hazard applications: Method, results, and limitations. *Natural Hazards*, 52(3), 561–575. <https://doi.org/10.1007/s11069-009-9401-4>
- Kitoh, A. (2017). The Asian monsoon and its future change in climate models: A review. *Journal of the Meteorological Society of Japan*, 95(1), 7–33. <https://doi.org/10.2151/jmsj.2017.002>

- Klein, J. A., Tucker, C. M., Steger, C. E., Nolin, A., Reid, R., Hopping, K. A., et al. (2019). An integrated community and ecosystem-based approach to disaster risk reduction in mountain systems. *Environmental Science & Policy*, *94*, 143–152. <https://doi.org/10.1016/j.envsci.2018.12.034>
- Kritikos, T., & Davies, T. (2015). Assessment of rainfall-generated shallow landslide/debris-flow susceptibility and runoff using a GIS-based approach: Application to western southern Alps of New Zealand. *Landslides*, *12*(6), 1051–1075. <https://doi.org/10.1007/s10346-014-0533-6>
- Kritikos, T., Robinson, T. R., & Davies, T. R. (2015). Regional coseismic landslide hazard assessment without historical landslide inventories: A new approach. *Journal of Geophysical Research: Earth Surface*, *120*(4), 711–729. <https://doi.org/10.1002/2014jf003224>
- Lennartz, T. (2013). Constructing roads—Constructing risks? Settlement decisions in view of landslide risk and economic opportunities in western Nepal. *Mountain Research and Development*, *33*(4), 364–371. <https://doi.org/10.1659/mrd-journal-d-13-00048.1>
- Maharjan, S. B., Steiner, J. F., Shrestha, A. B., Maharjan, A., Nepal, S., Singh Shrestha, M., et al. (2021). *The Melamchi flood disaster: Cascading hazard and the need for multihazard risk management*. ICIMOD. Retrieved from <https://lib.icimod.org/record/35284>
- Manchado, A. M.-T., Allen, S. K., Ballesteros Canovas, J. A., Dhakal, A., Dhital, M. R., & Stoffel, M. (2021). Three decades of landslide activity in western Nepal: New insights into trends and climate drivers. *Landslides*, *18*(6), 2001–2015. <https://doi.org/10.1007/s10346-021-01632-6>
- McAdoo, B. G., Quak, M., Gnyawali, K. R., Adhikari, B. R., Devkota, S., Rajbhandari, P. L., & Sudmeier-Rieux, K. (2018). Roads and landslides in Nepal: How development affects environmental risk. *Natural Hazards and Earth System Sciences*, *18*(12), 3203–3210. <https://doi.org/10.5194/nhess-18-3203-2018>
- McSweeney, C. F., Jones, R. G., & Booth, B. B. (2012). Selecting ensemble members to provide regional climate change information. *Journal of Climate*, *25*(20), 7100–7121. <https://doi.org/10.1175/jcli-d-11-00526.1>
- Meena, S. R., Albrecht, F., Hölbling, D., Ghorbanzadeh, O., & Blaschke, T. (2021). Nepalese landslide information system (NELIS): A conceptual framework for a web-based geographical information system for enhanced landslide risk management in Nepal. *Natural Hazards and Earth System Sciences*, *21*(1), 301–316. <https://doi.org/10.5194/nhess-21-301-2021>
- METEOR Project Consortium. (2020). Level 1 exposure data in csv format with OED codes [Dataset]. Modelling Exposure Through Earth Observation Routines (METEOR) Project Consortium. Retrieved from https://downloads.openquake.org/meteor/level1exposure/NPL_oes_exposure_20200811.zip
- Meunier, P., Hovius, N., & Haines, J. A. (2008). Topographic site effects and the location of earthquake induced landslides. *Earth and Planetary Science Letters*, *275*(3–4), 221–232. <https://doi.org/10.1016/j.epsl.2008.07.020>
- Milledge, D. G., Densmore, A. L., Bellugi, D., Rosser, N. J., Watt, J., Li, G., & Owen, K. J. (2019). Simple rules to minimise exposure to coseismic landslide hazard. *Natural Hazards and Earth System Sciences*, *19*(4), 837–856. <https://doi.org/10.5194/nhess-19-837-2019>
- Monsieurs, E., Jacobs, L., Michellier, C., Tchangaboba, J. B., Ganz, G. B., Kervyn, F., et al. (2018). Landslide inventory for hazard assessment in a data-poor context: A regional-scale approach in a tropical African environment. *Landslides*, *15*(11), 2195–2209. <https://doi.org/10.1007/s10346-018-1008-y>
- Nadim, F., Kjekstad, O., Peduzzi, P., Herold, C., & Jaedicke, C. (2006). Global landslide and avalanche hotspots. *Landslides*, *3*(2), 159–173. <https://doi.org/10.1007/s10346-006-0036-1>
- Neupane, S. (2020). *BIPAD for decision making in federal Nepal*. Youth Innovation Lab. Retrieved from https://www.preventionweb.net/files/73985_73985bipadfordecisionmakinginfedera.pdf
- Oven, K. (2009). *Landscape, livelihoods and risk: Community vulnerability to landslides in Nepal (Doctoral thesis)*. Durham University. Retrieved from <http://theses.dur.ac.uk/183/>
- Oven, K., Rana, S., Basyal, G. K., & Rosser, N. (2021). Policies, politics, and practices of landslide risk management in post-earthquake Nepal. In *Epicentre to aftermath: Rebuilding and remembering in the wake of Nepal's earthquakes* (p. 151).
- Oven, K., & Rigg, J. D. (2015). The best of intentions? Managing disasters and constructions of risk and vulnerability in Asia. *Asian Journal of Social Science*, *43*(6), 685–712. <https://doi.org/10.1163/15685314-04306003>
- Ozturk, U., Pittore, M., Behling, R., Roessner, S., Andreani, L., & Korup, O. (2021). How robust are landslide susceptibility estimates? *Landslides*, *18*(2), 681–695. <https://doi.org/10.1007/s10346-020-01485-5>
- Parker, R. N., Hancox, G. T., Petley, D. N., Massey, C. I., Densmore, A. L., & Rosser, N. J. (2015). Spatial distributions of earthquake-induced landslides and hillslope preconditioning in the northwest South Island, New Zealand. *Earth Surface Dynamics*, *3*(4), 501–525. <https://doi.org/10.5194/esurf-3-501-2015>
- Pellicani, R., Van Westen, C. J., & Spilotro, G. (2014). Assessing landslide exposure in areas with limited landslide information. *Landslides*, *11*(3), 463–480. <https://doi.org/10.1007/s10346-013-0386-4>
- Persichillo, M. G., Bordoni, M., Meisina, C., Bartelletti, C., Barsanti, M., Gianecchini, R., et al. (2017). Shallow landslides susceptibility assessment in different environments. *Geomatics, Natural Hazards and Risk*, *8*(2), 748–771. <https://doi.org/10.1080/19475705.2016.1265011>
- Petley, D. (2012). Global patterns of loss of life from landslides. *Geology*, *40*(10), 927–930. <https://doi.org/10.1130/g33217.1>
- Petley, D. N., Hearn, G. J., Hart, A., Rosser, N. J., Dunning, S. A., Oven, K., & Mitchell, W. A. (2007). Trends in landslide occurrence in Nepal. *Natural Hazards*, *43*(1), 23–44. <https://doi.org/10.1007/s11069-006-9100-3>
- Petschko, H., Brenning, A., Bell, R., Goetz, J., & Glade, T. (2014). Assessing the quality of landslide susceptibility maps—case study lower Austria. *Natural Hazards and Earth System Sciences*, *14*(1), 95–118. <https://doi.org/10.5194/nhess-14-95-2014>
- Pourghasemi, H. R., Pradhan, B., & Gokceoglu, C. (2012). Application of fuzzy logic and analytical hierarchy process (AHP) to landslide susceptibility mapping at Haraz watershed, Iran. *Natural Hazards*, *63*(2), 965–996. <https://doi.org/10.1007/s11069-012-0217-2>
- Pradhan, B. (2010). Landslide susceptibility mapping of a catchment area using frequency ratio, fuzzy logic and multivariate logistic regression approaches. *Journal of the Indian Society of Remote Sensing*, *38*(2), 301–320. <https://doi.org/10.1007/s12524-010-0020-z>
- Promper, C., Gassner, C., & Glade, T. (2015). Spatiotemporal patterns of landslide exposure—a step within future landslide risk analysis on a regional scale applied in Waidhofen/Ybbs Austria. *International Journal of Disaster Risk Reduction*, *12*, 25–33. <https://doi.org/10.1016/j.ijdrr.2014.11.003>
- Reichenbach, P., Rossi, M., Malamud, B. D., Mihir, M., & Guzzetti, F. (2018). A review of statistically-based landslide susceptibility models. *Earth-Science Reviews*, *180*, 60–91. <https://doi.org/10.1016/j.earscirev.2018.03.001>
- Rieger, K. (2021). Multi-hazards, displaced people's vulnerability and resettlement: Post-earthquake experiences from Rasuwa district in Nepal and their connections to policy loopholes and reconstruction practices. *Progress in Disaster Science*, *11*, 100187. <https://doi.org/10.1016/j.pdisas.2021.100187>
- Robinson, T. R., Rosser, N. J., Densmore, A. L., Williams, J. G., Kincey, M. E., Benjamin, J., & Bell, H. J. (2017). Rapid post-earthquake modelling of coseismic landslide intensity and distribution for emergency response decision support. *Natural Hazards and Earth System Sciences*, *17*(9), 1521–1540. <https://doi.org/10.5194/nhess-17-1521-2017>
- Rosser, N., Kincey, M., Oven, K., Densmore, A., Robinson, T., Pujara, D. S., et al. (2021). Changing significance of landslide Hazard and risk after the 2015 Mw 7.8 Gorkha, Nepal earthquake. *Progress in Disaster Science*, *10*, 100159. <https://doi.org/10.1016/j.pdisas.2021.100159>

- Rusk, J., Maharjan, A., Tiwari, P., Chen, T. H. K., Shneiderman, S., Turin, M., & Seto, K. C. (2022). Multi-hazard susceptibility and exposure assessment of the Hindu Kush Himalaya. *Science of the Total Environment*, 804, 150039. <https://doi.org/10.1016/j.scitotenv.2021.150039>
- Schwanghart, W., Ryan, M., & Korup, O. (2018). Topographic and seismic constraints on the vulnerability of Himalayan hydropower. *Geophysical Research Letters*, 45(17), 8985–8992. <https://doi.org/10.1029/2018gl079173>
- Shugar, D. H., Jacquemart, M., Shean, D., Bhushan, S., Upadhyay, K., Sattar, A., et al. (2021). A massive rock and ice avalanche caused the 2021 disaster at Chamoli, Indian Himalaya. *Science*, 373(6552), 300–306. <https://doi.org/10.1126/science.abh4455>
- Sidle, R. C., Gallina, J., & Gomi, T. (2017). The continuum of chronic to episodic natural hazards: Implications and strategies for community and landscape planning. *Landscape and Urban Planning*, 167, 189–197. <https://doi.org/10.1016/j.landurbplan.2017.05.017>
- Smyth, C. G., & Royle, S. A. (2000). Urban landslide hazards: Incidence and causative factors in Niterói, Rio de Janeiro State, Brazil. *Applied Geography*, 20(2), 95–118. [https://doi.org/10.1016/s0143-6228\(00\)00004-7](https://doi.org/10.1016/s0143-6228(00)00004-7)
- Stanley, T., & Kirschbaum, D. B. (2017). A heuristic approach to global landslide susceptibility mapping. *Natural Hazards*, 87(1), 145–164. <https://doi.org/10.1007/s11069-017-2757-y>
- Stein, S., Brooks, E. M., Spencer, B. D., & Liu, M. (2018). Should all of Nepal be treated as having the same earthquake hazard? In *Living under the threat of earthquakes* (pp. 27–44). Springer.
- Stevens, F. R., Gaughan, A. E., Linard, C., & Tatem, A. J. (2015). Disaggregating census data for population mapping using random forests with remotely-sensed and ancillary data. *PLoS One*, 10(2), e0107042. <https://doi.org/10.1371/journal.pone.0107042>
- Sudmeier-Rieux, K., Gaillard, J. C., Sharma, S., Dubois, J., & Jaboyedoff, M. (2012). Floods, landslides, and adapting to climate change in Nepal: What role for climate change models? In A. Lamadrid & I. Kelman (Eds.), *Climate change modeling for local adaptation in the Hindu Kush-Himalayan Region*. Emerald Group Publishing Limited.
- Sudmeier-Rieux, K., McAdoo, B. G., Devkota, S., Rajbhandari, P. C. L., Howell, J., & Sharma, S. (2019). Invited perspectives: Mountain roads in Nepal at a new crossroads. *Natural Hazards and Earth System Sciences*, 19(3), 655–660. <https://doi.org/10.5194/nhess-19-655-2019>
- Tatem, A. J. (2017). WorldPop, open data for spatial demography. *Scientific Data*, 4(1), 1–4. <https://doi.org/10.1038/sdata.2017.4>
- Tobin, G. A., Whiteford, L. M., Jones, E. C., Murphy, A. D., Garren, S. J., & Padros, C. V. (2011). The role of individual well-being in risk perception and evacuation for chronic vs. acute natural hazards in Mexico. *Applied Geography*, 31(2), 700–711. <https://doi.org/10.1016/j.apgeog.2010.12.008>
- TReNDS. (2020). Leaving no one off the map: A guide for gridded population data for sustainable development. A report by the thematic research network on data and statistics (TReNDS) of the UN sustainable development solutions network (SDSN). Retrieved from <https://static1.squarespace.com/static/5b4f63e14eddec374f416232t/5eb2b65ec575060f0adb1feb/1588770424043/>
- UNISDR. (2015). Making development sustainable: The future of disaster risk management. In *Global assessment report on disaster risk reduction*. United Nations Office for Disaster Risk Reduction.
- Wester, P., Mishra, A., Mukherji, A., & Shrestha, A. B. (2019). *The Hindu Kush Himalaya assessment: Mountains, climate change, sustainability and people* (p. 627). Springer Nature.
- WorldPop (2020). The spatial distribution of population in 2011 with country total adjusted to match the corresponding UNPD estimate, Nepal [Dataset]. School of Geography and Environmental Science, University of Southampton; Department of Geography and Geosciences, University of Louisville; Departement de Geographie, Universite de Namur and Center for International Earth Science Information Network (CIESIN), Columbia University (2018). Global High Resolution Population Denominators Project - Funded by The Bill and Melinda Gates Foundation (OPP1134076). <https://doi.org/10.5258/SOTON/WP00660>
- Wymann von Dach, S., Bachmann, F., Alcántara-Ayala, I., Fuchs, S., Keiler, M., Mishra, A., et al. (Eds.) (2017). *Safer lives and livelihoods in mountains: Making the Sendai Framework for Disaster Risk Reduction work for sustainable mountain development* (p. 78). Centre for Development and Environment (CDE), University of Bern, with Bern Open Publishing (BOP). Retrieved from <https://www.preventionweb.net/publication/safer-lives-and-livelihoods-mountains-making-sendai-framework-disaster-risk-reduction>
- Ziegler, A. D., Wasson, R. J., Bhardwaj, A., Sundriyal, Y. P., Sati, S. P., Juyal, N., et al. (2014). Pilgrims, progress, and the political economy of disaster preparedness—the example of the 2013 Uttarakhand flood and Kedarnath disaster. *Hydrological Processes*, 28(24), 5985–5990. <https://doi.org/10.1002/hyp.10349>
- Zimmermann, M., & Keiler, M. (2015). International frameworks for disaster risk reduction: Useful guidance for sustainable mountain development? *Mountain Research and Development*, 35(2), 195–202. <https://doi.org/10.1659/MRD-JOURNAL-D-15-00006.1>

References From the Supporting Information

- Aleotti, P., & Chowdhury, R. (1999). Landslide hazard assessment: Summary review and new perspectives. *Bulletin of Engineering Geology and the Environment*, 58(1), 21–44. <https://doi.org/10.1007/s100640050066>
- Catani, F., Casagli, N., Ermini, L., Righini, G., & Menduni, G. (2005). Landslide hazard and risk mapping at catchment scale in the Arno River basin. *Landslides*, 2(4), 329–342. <https://doi.org/10.1007/s10346-005-0021-0>
- Catani, F., Segoni, S., & Falorni, G. (2010). An empirical geomorphology-based approach to the spatial prediction of soil thickness at catchment scale. *Water Resources Research*, 46(5), W05508. <https://doi.org/10.1029/2008wr007450>
- Catani, F., Lagomarsino, D., Segoni, S., & Tofani, V. (2013). Landslide susceptibility estimation by random forests technique: Sensitivity and scaling issues. *Natural Hazards and Earth System Sciences*, 13(11), 2815–2831. <https://doi.org/10.5194/nhess-13-2815-2013>
- Costanzo, D., Rotigliano, E., Irigaray, C., Jiménez-Perálvarez, J. D., & Chacón, J. (2012). Factors selection in landslide susceptibility modelling on large scale following the gis matrix method: Application to the river Beiro basin (Spain). *Natural Hazards and Earth System Sciences*, 12(2), 327–340. <https://doi.org/10.5194/nhess-12-327-2012>
- Dai, F. C., & Lee, C. F. (2002). Landslide characteristics and slope instability modeling using GIS, Lantau Island, Hong Kong. *Geomorphology*, 42(3–4), 213–228. [https://doi.org/10.1016/s0169-555x\(01\)00087-3](https://doi.org/10.1016/s0169-555x(01)00087-3)
- Demir, G., Aytikin, M., Akgün, A., İkizler, S. B., & Tatar, O. (2013). A comparison of landslide susceptibility mapping of the eastern part of the North Anatolian Fault Zone (Turkey) by likelihood-frequency ratio and analytic hierarchy process methods. *Natural Hazards*, 65(3), 1481–1506. <https://doi.org/10.1007/s11069-012-0418-8>
- Devkota, K. C., Regmi, A. D., Pourghasemi, H. R., Yoshida, K., Pradhan, B., Ryu, I. C., et al. (2013). Landslide susceptibility mapping using certainty factor, index of entropy and logistic regression models in GIS and their comparison at Mugling–Narayanghat road section in Nepal Himalaya. *Natural Hazards*, 65(1), 135–165. <https://doi.org/10.1007/s11069-012-0347-6>
- Evans, I. S. (1998). What do terrain statistics really mean? In S. N. Lane, K. S. Richards, & J. H. Chandler (Eds.), *Landform monitoring, modelling and analysis* (pp. 119–138). Wiley.

- Felicísimo, Á. M., Cuartero, A., Remondo, J., & Quirós, E. (2013). Mapping landslide susceptibility with logistic regression, multiple adaptive regression splines, classification and regression trees, and maximum entropy methods: A comparative study. *Landslides*, *10*(2), 175–189. <https://doi.org/10.1007/s10346-012-0320-1>
- Frattini, P., Crosta, G., & Carrara, A. (2010). Techniques for evaluating the performance of landslide susceptibility models. *Engineering Geology*, *111*(1–4), 62–72. <https://doi.org/10.1016/j.enggeo.2009.12.004>
- Guzzetti, F., Carrara, A., Cardinali, M., & Reichenbach, P. (1999). Landslide hazard evaluation: A review of current techniques and their application in a multi-scale study, Central Italy. *Geomorphology*, *31*(1–4), 181–216. [https://doi.org/10.1016/s0169-555x\(99\)00078-1](https://doi.org/10.1016/s0169-555x(99)00078-1)
- Günther, A., Reichenbach, P., Malet, J. P., Van Den Eeckhaut, M., Hervás, J., Dashwood, C., & Guzzetti, F. (2013). Tier-based approaches for landslide susceptibility assessment in Europe. *Landslides*, *10*(5), 529–546. <https://doi.org/10.1007/s10346-012-0349-1>
- Kayastha, P., Dhital, M. R., & De Smedt, F. (2012). Landslide susceptibility mapping using the weight of evidence method in the Tinau watershed, Nepal. *Natural Hazards*, *63*(2), 479–498. <https://doi.org/10.1007/s11069-012-0163-z>
- Oguchi, T. (1997). Drainage density and relative relief in humid steep mountains with frequent slope failure. *Earth Surface Processes and Landforms*, *22*(2), 107–120. [https://doi.org/10.1002/\(sici\)1096-9837\(199702\)22:2<107::aid-esp680>3.0.co;2-u](https://doi.org/10.1002/(sici)1096-9837(199702)22:2<107::aid-esp680>3.0.co;2-u)
- Ohlmacher, G. C. (2007). Plan curvature and landslide probability in regions dominated by earth flows and earth slides. *Engineering Geology*, *91*(2–4), 117–134. <https://doi.org/10.1016/j.enggeo.2007.01.005>
- Pereira, S., Zêzere, J. L., & Bateira, C. (2012). Assessing predictive capacity and conditional independence of landslide predisposing factors for shallow landslide susceptibility models. *Natural Hazards and Earth System Sciences*, *12*(4), 979–988. <https://doi.org/10.5194/nhess-12-979-2012>
- Sabatakakis, N., Koukis, G., Vassiliades, E., & Lainas, S. (2013). Landslide susceptibility zonation in Greece. *Natural Hazards*, *65*(1), 523–543. <https://doi.org/10.1007/s11069-012-0381-4>
- Sudmeier-Rieux, K., Jaquet, S., Derron, M. H., Jaboyedoff, M., & Devkota, S. (2012). A case study of coping strategies and landslides in two villages of Central-Eastern Nepal. *Applied Geography*, *32*(2), 680–690. <https://doi.org/10.1016/j.apgeog.2011.07.005>
- Xu, C., Xu, X., Dai, F., Wu, Z., He, H., Shi, F., et al. (2013). Application of an incomplete landslide inventory, logistic regression model and its validation for landslide susceptibility mapping related to the May 12, 2008 Wenchuan earthquake of China. *Natural Hazards*, *68*(2), 883–900. <https://doi.org/10.1007/s11069-013-0661-7>
- Zevenbergen, L. W., & Thorne, C. R. (1987). Quantitative analysis of land surface topography. *Earth Surface Processes and Landforms*, *12*(1), 47–56. <https://doi.org/10.1002/esp.3290120107>